

This is an Accepted Manuscript of the following article:

A. Liland, O.C. Lind, J. Bartnicki, J.E. Brown, J.E. Dyve,  
M. Iosjpe, H. Kleine, Y. Lin, M. Simonsen, P. Strand, H.  
Thørring, M.A. Ytre-Eide, B. Salbu.

Using a chain of models to predict health and environmental impacts in  
Norway from a hypothetical nuclear accident at the Sellafield site.

Journal of Environmental Radioactivity.  
214-215, 2020, 106159, ISSN 0265-931X.

The article has been published in final form by Elsevier at  
<http://dx.doi.org/10.1016/j.jenvrad.2020.106159>

© 2020. This manuscript version is made available under the

CC-BY-NC-ND 4.0 license

<http://creativecommons.org/licenses/by-nc-nd/4.0/>

---

# 1 Using a chain of models to predict health and environmental impacts in Norway from a 2 hypothetical nuclear accident at the Sellafield site

3

4 Keywords: nuclear accidents; radioactive fallout; multi-compartment modelling; decision  
5 support systems; model uncertainties

## 6 1 Introduction

7 When a nuclear accident occurs, decision makers in the affected country/countries would  
8 need to act promptly to protect people, the environment and societal interests from harmful  
9 impacts of radioactive fallout. The decisions are usually based on a combination of model  
10 prognoses, measurements, and expert judgements within in an emergency preparedness  
11 framework. Following the Chernobyl accident, several decision support systems (DSS) were  
12 developed in Europe to provide expert support to decision makers should a nuclear accident  
13 occur. The DSS have been expanded over the years to include an increasing number of  
14 modules with specific functions for various ecosystems. The early atmospheric dispersion  
15 and deposition models had subsequent food chain contamination modules and dose  
16 calculations for humans, while some DSS now include modules for urban, forest and aquatic  
17 environments as well as countermeasures in various ecosystems, e.g., ERMIN (European  
18 Model for Inhabited Areas) and AgriCP (Agricultural Countermeasure Programme) (Raskob  
19 et al., 2010). In the event of radioactive fallout, there would be a subsequent transfer of  
20 radionuclides between different environmental compartments due to e.g., erosion, run-off,  
21 forestry and agricultural practice, and from rivers via estuaries to the marine ecosystems.  
22 This environmental transfer of radionuclides and the radiation exposures of humans and biota  
23 should be assessed to determine whether protective actions and/or remediation would be  
24 necessary. Thus, predictive models would need to cover the atmospheric, terrestrial,  
25 freshwater, and marine ecosystems, the connections between these in terms of radionuclide

26 fluxes and the various exposure pathways to both humans and biota. This could be achieved  
27 by coupling different ecosystem models either as stand-alone models used in a chain or as  
28 linked modules within a nuclear decision support system like ARGOS (Accident Reporting  
29 and Guiding Operational System) (Hoe et al., 2009) or RODOS (Real Time On-line Decision  
30 Support) (Landman et al., 2014). The results obtained could be further used in optimising  
31 countermeasure strategies and performing cost-benefit analyses for remediation.

32 As DSS are necessarily generic in character, regional or country specific predictions  
33 can be improved by adapting model configurations and through bespoke parametrization.  
34 However, this could be an elaborate and time-consuming process. Alternatively, already  
35 existing national or regional models may be applied instead, either alone or in combination  
36 with certain modules of DSS.

37 As pointed out by Salbu (2016) integrated models for impact and risk assessments are  
38 complex systems and the predictive model output is confounded by uncertainties that stem  
39 from various sources. She categorized the sources of uncertainties accordingly:

- 40 (1) *Input uncertainty* (experimental uncertainties);
- 41 (2) *Interpolation and extrapolation uncertainty* (due to insufficient or lacking input data);
- 42 (3) *Parameter uncertainty and variability* (inherent variability and parameter values that  
43 cannot be experimentally controlled);
- 44 (4) *Algorithmic uncertainty* (numerical errors and approximations in the mathematical  
45 model); and
- 46 (5) *Structural uncertainty*.

47 The latter, also referred to as conceptual or model uncertainty, is assigned to model bias or  
48 discrepancy from real life due to lack of knowledge or to deliberate omission of relevant  
49 mechanisms, processes or phenomena.

50 Reducing uncertainties in predictive models is one of the key aims of the Norwegian  
51 Centre of Excellence for Environmental Radioactivity (CERAD CoE)<sup>1</sup> to underpin the core  
52 objective of providing the scientific basis for impact and risk assessments in management of  
53 radiation risks, both for past events and for potential future events. CERAD initiated this case  
54 study to assess possible human and environmental impacts in Norway from a hypothetical  
55 accident at the Sellafield nuclear reprocessing plant using a range of models. The study had  
56 two distinct goals:

57 (a) To investigate if selected regional/local models and DSS could be linked in a meaningful  
58 way to predict impacts in relevant ecosystems from nuclear accidents and to test the linked  
59 models for a hypothetical accident with radioactive fallout in Norway.

60 (b) To identify key factors contributing to the uncertainties in predictive model outputs, and  
61 to decide, based on sensitivity analyses as well as expert judgement, which key factors to  
62 focus on in further research.

63

## 64 2 Methods and models

### 65 2.1 Scope

66 A combination of the ARGOS DSS with modules and other predictive models were  
67 used to assess the impacts for several ecosystems of a hypothetical accident at the Sellafield  
68 nuclear reprocessing plant. Table 1 presents the names of the DSS, modules and models used  
69 and their application. A generic description of each model is given in Appendix 1.

70

71 *Table 1: Overview of the DSS, modules and models used to assess the impacts in Norway from a hypothetical accident*  
72 *scenario at the Sellafield site.*

---

<sup>1</sup> <https://www.nmbu.no/en/services/centers/cerad/node/24335>

Short name	Full name	Application
SNAP	Severe Nuclear Accident Programme	Atmospheric dispersion and deposition of radionuclides
ARGOS	Accident Reporting and Guiding Operational System	Decision support system for nuclear and radiological accidents, external and inhalation doses to humans
FDMT	Food Chain and Dose Module - Terrestrial	Concentrations of radionuclides in food and feed, ingestion doses to humans
STRATOS	N/A	Concentrations of radionuclides in wild foodstuffs and rough grazing animals' products
INCA-RAD	INtegrated CAatchment model for RADionuclides	Transport and retention of radionuclides in freshwater systems
NRPA marine box model	N/A	Dispersion of radionuclides in marine waters, concentrations in and dose rates to marine biota
ROMS	Regional Ocean Model System	Dynamic dispersion of radionuclides in marine waters
ERICA Tool	N/A	Concentrations of radionuclides in biota, dose rates to biota, environmental risk assessment

73

74

75

76

77

78

79

80

81

82

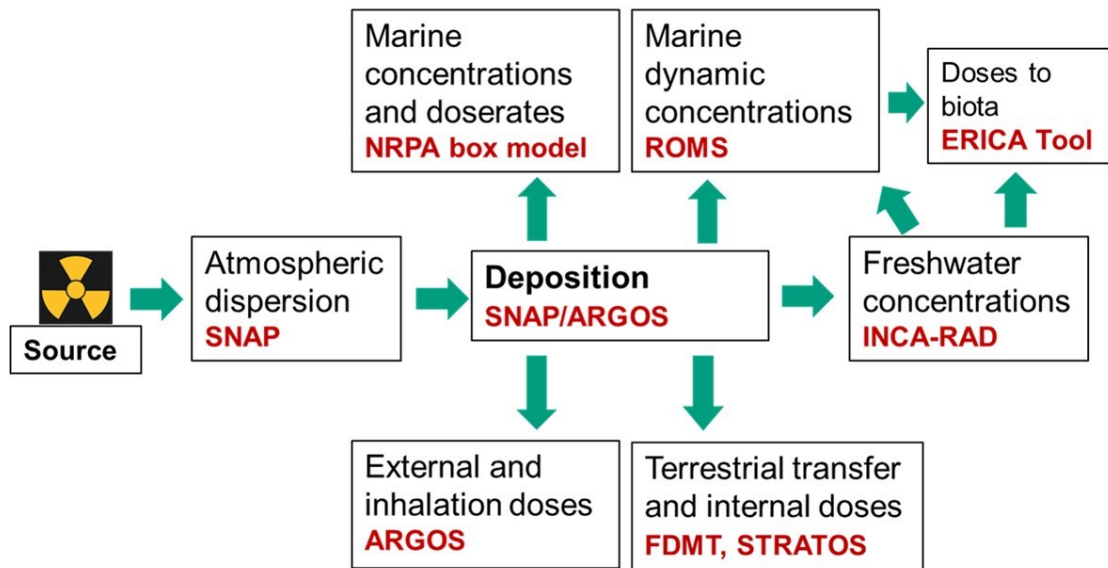
83

84

85

86

Figure 1 shows how the models were linked. Based on an estimated inventory of  $^{137}\text{Cs}$ , an accident source term and a real meteorological scenario, the SNAP (Severe Nuclear Accident Programme) model was used to simulate atmospheric dispersion and transport of radionuclides to Norway. Total deposition maps of  $^{137}\text{Cs}$  were produced for marine, freshwater and terrestrial areas. ARGOS DSS estimated external and inhalation doses to humans while the contamination of agricultural produce and ingestion doses to humans were calculated using its module FDMT (Terrestrial Food Chain and Dose Module). For wild foodstuff and rough grazing animals, the STRATOS model was used to predict areas where food intervention levels might be exceeded. INCA-RAD (INtegrated CAatchment model for RADionuclides) modelled contamination in freshwater bodies from direct deposition and catchment run-off. Two models were used for the marine ecosystem: the NRPA marine box model and the dynamic Regional Ocean Model System (ROMS). The ERICA Tool was used to calculate concentrations in and dose rates to aquatic species.



87

88 *Figure 1: Linking the different DSS, modules and models in a chain to assess impacts.*

## 89 **2.2 Hypothetical accident scenario at the Sellafield nuclear reprocessing plant**

### 90 **2.2.1 Inventory and source term**

91 The Sellafield nuclear site, situated on the coast of the Irish Sea in Cumbria, England,  
 92 is currently owned by the Nuclear Decommissioning Authority (NDA) and operated by  
 93 Sellafield Ltd. One of the main activities has been reprocessing of spent nuclear fuel during  
 94 which uranium and plutonium were recovered for producing mixed oxide fuel. The  
 95 reprocessing resulted in large volumes of highly active liquor (HAL) as a waste by-product.  
 96 This HAL is temporarily stored in 21 specially designed tanks (Highly Active Storage Tanks  
 97 - HASTs) until the waste can be vitrified, i.e., blended as part of a solid glass matrix that is  
 98 easier to handle and safer for long-term storage. The HAL produces heat and needs  
 99 continuous cooling to avoid the liquid to evaporate. The inventory in the HASTs was  
 100 calculated to be approximately  $1.9 - 3.0 \cdot 10^{18}$  Bq for  $^{137}\text{Cs}$  as of April 2014 (see Appendix 2  
 101 for calculations).

102 The HASTs constitute a potential threat for contaminating the environment either due to  
103 failure of the cooling system, a natural disaster (e.g., earthquake) or a malevolent act (e.g.,  
104 bomb, plane crash) that would destroy the integrity of the tanks. Indeed, in 1957 in Kysthym,  
105 Soviet Union, the cooling system of a similar waste storage tank from the Mayak Production  
106 Facility failed and evaporation of the cooling liquid resulted in a chemical explosion. It  
107 resulted in a loss of the tank`s integrity and vast amounts of radioactive material (in the order  
108 of PBq) were emitted to the atmosphere, contaminating a large area (Norwegian Radiation  
109 Protection Authority, 2007). Furthermore, historic discharges from Sellafield to the marine  
110 environment have contaminated the Norwegian coastline for many years. Combined with  
111 concerns over nuclear safety at the site, Sellafield Ltd has been of concern to Norwegian  
112 authorities, NGOs and the public for a long time (Liland et al., 2017).

113 We have deliberately not estimated the probability of a possible accident release  
114 scenario, be it the loss of cooling, a natural disaster or a malevolent act. We simply assume a  
115 scenario with a loss of the HAL tanks` integrity and that 1 % of the estimated  $^{137}\text{Cs}$  in the  
116 tanks ( $3.0 \cdot 10^{16}$  Bq) is released to the air as aerosols at a height where it can be mixed with the  
117 atmosphere and then transported to Norway by atmospheric dispersion. 1% is not an  
118 unreasonable estimate according to an earlier study by Ytre-Eide et al. (2009): “The UK  
119 Parliamentary Office of Science and Technology observe that earlier impact assessments ...  
120 have used quite different source terms; from 0.01 % of one HAST inventory to over 10 % of  
121 all the HASTs contents”.

122 The tanks also contain other long-lived radionuclides such as  $^{90}\text{Sr}$ ,  $^{241}\text{Am}$  and  $^{244}\text{Cm}$ ,  
123 but this study is restricted to only include  $^{137}\text{Cs}$ . There are no short-lived radionuclides  
124 present in the HAL.

125

## 126 **2.2.2 Meteorological scenario**

127         The selected meteorological scenario was based on real weather data recorded in  
128 October 2008 (Ytre-Eide et al., 2009) and the hypothetical accident was assumed to have  
129 occurred on 19 October 2008 at 13:00 UTC. The weather situation at that time was  
130 dominated by a low pressure system located southeast of Iceland. This caused southwest  
131 winds towards Scandinavia across the North Sea with extensive precipitation in the south-  
132 western part of Norway. The precipitation in Bergen, the largest city on the west coast, was  
133 20, 15 and 30 mm of rainfall for 19, 20 and 21 October, respectively. The Norwegian  
134 Meteorological Institute (MET Norway) considered this weather to be representative for this  
135 season and geographical region. Under such circumstances a potential radioactive release  
136 could reach the Norwegian coast within a period of nine hours from the release time (Ytre-  
137 Eide et al., 2009).

## 138 **2.3 Linking the models**

### 139 **2.3.1 Atmospheric dispersion and deposition, doses to humans**

140         Atmospheric dispersion from the site of accident was modelled by SNAP based on the  
141 inventory and source term as described in chapter 2.2 and Appendix 2 and using  
142 meteorological data from the HIRLAM model (see Appendix A.1.1 for details). The  
143 emissions were considered to have a duration of 5 minutes, consistent with e.g., an explosion.  
144 The emission height given as model input to the SNAP model refers to the height where  
145 model particles enter the atmosphere without being further disturbed by the source. This is  
146 not actually the stack-height of the source, but rather a combination of stack-height and  
147 plume rise. Our scenario used an emission height between 0 and 800 m. The model particles  
148 carrying  $^{137}\text{Cs}$  were assumed to be aerosols with density  $2.3 \text{ g cm}^{-3}$ .



149           The output from SNAP ( $\text{Bq}\cdot\text{h m}^{-3}$ ,  $\text{Bq m}^{-3}$ ,  $\text{Bq m}^{-2}$ ) was converted from a rotated earth  
150 projection used by the meteorological model to two projections: WGS84 and UTM zone 33N,  
151 the former extending further to the north, both in approx. 10 km grid resolution. This was  
152 used as input in ARGOS DSS for wet, dry and total deposition ( $\text{Bq m}^{-2}$ ) and precipitation ( $\text{kg}$   
153  $\text{m}^{-2}$ ). Then, ARGOS DSS could directly calculate external and inhalation doses to humans  
154 (mSv over a specified time period) from this input.

155

### 156 **2.3.2 Food chain modelling**

157           The ARGOS data on terrestrial deposition ( $\text{Bq m}^{-2}$ ) and air concentration ( $\text{Bq m}^{-3}$ )  
158 was used as input in FDMT and STRATOS to predict concentrations ( $\text{Bq kg}^{-1}$ ) in agricultural  
159 produce, and wild foodstuffs and rough grazing animals, respectively. FDMT combined the  
160 modelled concentrations in agricultural produce with dietary statistics to calculate internal  
161 doses to humans of various age groups (mSv over a specified time period). STRATOS  
162 combined the deposition data ( $\text{Bq m}^{-2}$ ) with aggregated transfer factors ( $\text{kg m}^{-2}$ ) to predict  
163 concentrations ( $\text{Bq kg}^{-1}$ ) in rough grazing animals and wild foodstuffs. This was further  
164 linked to grazing and hunting statistics and extent of wild foodstuffs to predict how much of  
165 the annual yield or production (%) would exceed the food intervention levels for each  
166 foodstuff.

167

### 168 **2.3.3 Freshwater modelling**

169           The SNAP raster files for terrestrial deposition ( $\text{Bq m}^{-2}$ ) was used as input in the  
170 INCA-RAD model. The deposition on lakes, streams and catchment areas were included and  
171 the transport of  $^{137}\text{Cs}$  from soils and run-off to river, riverine transport and sediment  
172 dynamics was modelled for the investigated site in western Norway based on hydrology and

173 land use. The outputs from INCA-RAD were flow ( $\text{m}^3 \text{s}^{-1}$ ), concentration in water ( $\text{Bq m}^{-3}$ )  
174 and concentration in sediments ( $\text{Bq kg}^{-1}$ ) in lakes, rivers and tributaries in the Vikedal area, in  
175 daily time steps.

176 The data on concentrations in water ( $\text{Bq m}^{-3}$ ) and sediments ( $\text{Bq kg}^{-1}$ ) were used as  
177 input in the ERICA Tool version 1.0 to calculate concentrations ( $\text{Bq kg}^{-1}$ ) and dose rates  
178 ( $\mu\text{Gy h}^{-1}$ ) to freshwater species.

179 The daily outflow of  $^{137}\text{Cs}$  from the river Vikedal to the estuary in Vindafjorden was  
180 also calculated as well as the monthly outflow of  $^{137}\text{Cs}$  from 21 other rivers along the  
181 Norwegian coast. These were used as additional point sources of  $^{137}\text{Cs}$  for marine modelling  
182 with ROMS (see below).

183

### 184 **2.3.2 Marine modelling**

185 The SNAP raster files for deposition onto sea surface ( $\text{Bq m}^{-2}$ ) were converted into  
186 total surface deposition for each affected box ( $\text{Bq per box}$ ) in the NRPA marine box model.  
187 This input was then used to calculate concentrations in seawater ( $\text{Bq m}^{-3}$ ) at different depths,  
188 concentrations in sediments and marine organisms ( $\text{Bq kg}^{-1}$ ), and corresponding dose rates to  
189 biota ( $\mu\text{Gy h}^{-1}$ ) over time.

190 In the dynamic ocean model ROMS, the SNAP raster files for sea surface deposition  
191 ( $\text{Bq m}^{-2}$ ) were imported directly and combined with the daily river discharge data from  
192 INCA-RAD ( $\text{Bq d}^{-1}$ ) as additional point sources to predict concentrations in water ( $\text{Bq m}^{-3}$ ) at  
193 different depths in daily time steps. The water concentrations were used as input in the  
194 ERICA Tool to calculate concentrations ( $\text{Bq kg}^{-1}$ ) and dose rates ( $\mu\text{Gy h}^{-1}$ ) to marine species.  
195

## 196 3 Modelling results

197 Our study showed that all the models/modules/DSS in Figure 1 could be linked in a  
198 meaningful way to predict impacts in various ecosystems in Norway from radioactive fallout.  
199 The normal assumptions and default values in the models described in Appendix 1 were used  
200 in the predictive modelling of impacts from the hypothetical accident at Sellafield Ltd. unless  
201 otherwise specified in the text below. It should be noted that all the modelling results below  
202 are given as additional  $^{137}\text{Cs}$  due to this hypothetical accident;  $^{137}\text{Cs}$  already present in the  
203 environment due to global fallout from atmospheric testing of nuclear weapons and fallout  
204 from the Chernobyl accident is not included.

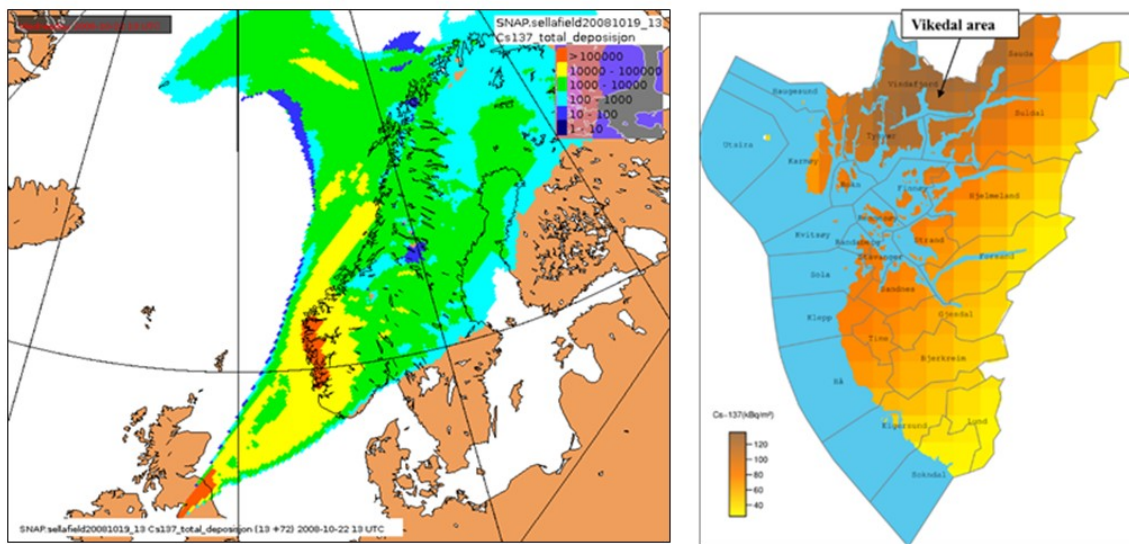
205

### 206 ***3.1 Simulated atmospheric dispersion and fallout in Norway - SNAP***

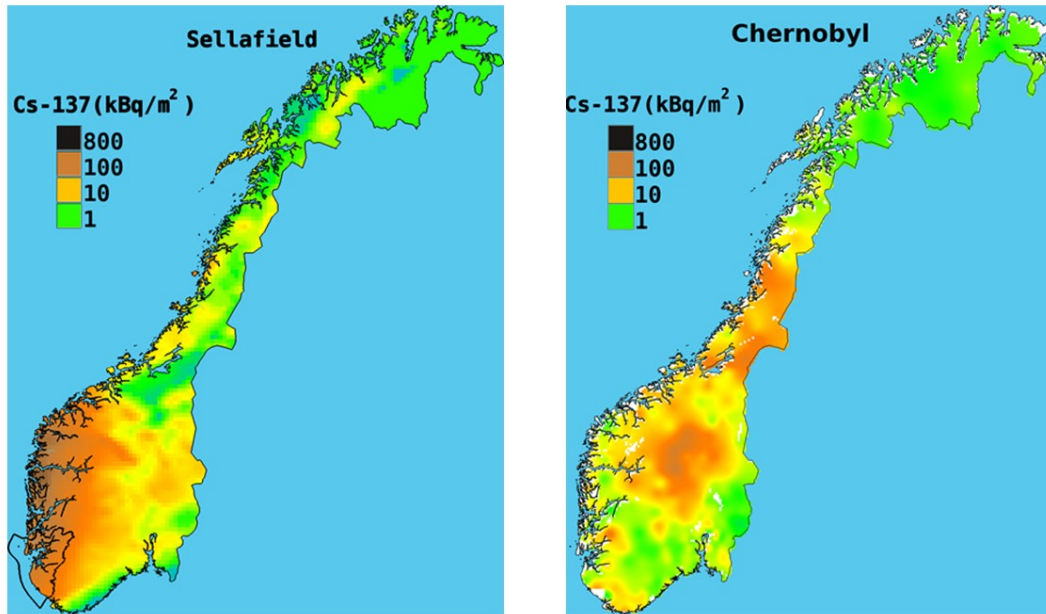
207 The atmospheric dispersion from the accident site and the subsequent fallout in  
208 Norway was simulated with the model SNAP (Figure 2, left). The model particles carrying  
209  $^{137}\text{Cs}$  were assumed to be solely aerosols of density  $2.3 \text{ g cm}^{-3}$ . We know, however, that  
210 releases from nuclear accidents could entail particles of various sizes and densities. This will  
211 influence on the simulated transport and deposition. The selection of an aerosol size and  $2.3 \text{ g}$   
212  $\text{cm}^{-3}$  density is considered to be a conservative approach, appropriate for a worst case  
213 scenario, since the lifetime for such particles in the atmosphere is relatively long, compared  
214 to other forms e.g., particles of a larger size (Klein et al., 2016).

215 The largest fallout for this hypothetical accident at Sellafield will occur on the western  
216 coast of Norway, with large areas predicted to be contaminated with  $^{137}\text{Cs}$  levels above  $100$   
217  $\text{kBq m}^{-2}$ . The simulated fallout levels are comparable to the most contaminated areas in  
218 Norway after the Chernobyl accident (Figure 3).

219 Of the most heavily contaminated areas in the hypothetical accident, the county of  
 220 Rogaland (see Figure 2, right) was selected for further impact assessments for several  
 221 reasons. It is the fourth most populated county in Norway with significant agricultural  
 222 production, fisheries, aquaculture and environmentally important areas. A radioactive fallout  
 223 in Rogaland would have substantial negative impacts on inhabitants, environment,  
 224 agriculture, aquaculture, fisheries, recreation and tourism. In addition, there is a general lack  
 225 of radiological data and impact assessments for this region since it was hardly affected by the  
 226 Chernobyl accident. The River Vikedal area in Vindafjord municipality, Rogaland was  
 227 selected to specifically study effects on the freshwater system since generic environmental  
 228 monitoring data covering several decades are available (Sandlund et al., 2010).



229  
 230 *Figure 2: Atmospheric dispersion and deposition of <sup>137</sup>Cs in Bq m<sup>-2</sup> during 24 h over Norwegian territories after a*  
 231 *hypothetical accident at the Sellafield HASTs using SNAP and presented in the visualisation programme DIANA (left). A*  
 232 *detailed map over the deposition (kBq m<sup>-2</sup>) in Rogaland County produced in GRASS GIS is shown on the right together with*  
 233 *the location of the Vikedal area (Liland et al., 2017).*

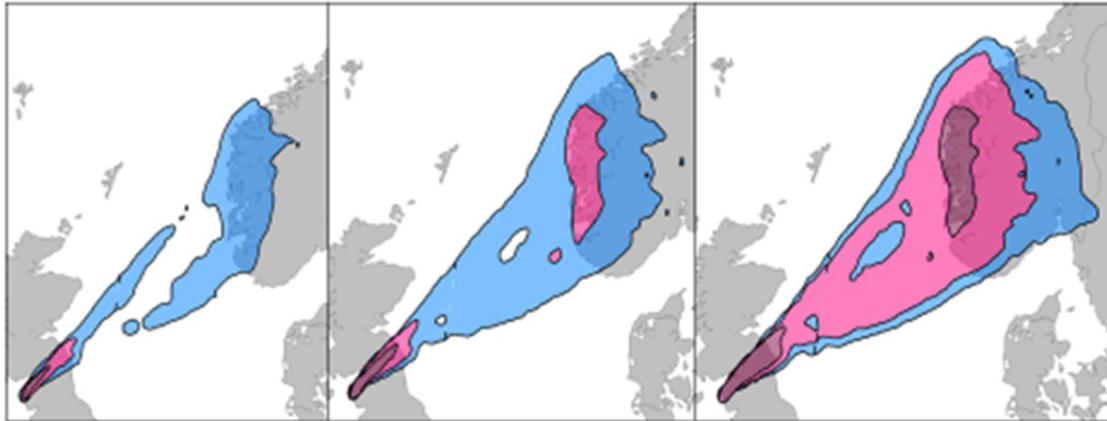


234  
 235 Figure 3: Compared fallout from the hypothetical accident at Sellafield (left) (Liland et al., 2017) and the Chernobyl  
 236 accident in 1986 (right) (Backe et al., 1986). Rogaland County is outlined in the south-western part of Norway on the left  
 237 figure.

### 238 3.2 External and inhalation doses to humans - ARGOS DSS

239 The total effective dose to adult humans from inhalation and external exposure to  
 240  $^{137}\text{Cs}$  after one week, one month and one year was calculated in ARGOS and is presented in  
 241 Figure 4. The highest average outdoor dose modelled in Norway was 2.7 mSv over the first  
 242 year. This is a conservative estimate calculated on the basis that people stay outdoors all the  
 243 time. In real life, people would be less exposed as buildings will provide substantial shielding  
 244 to external doses (Komperød et al., 2015). According to the Nordic guidelines and  
 245 recommendations (2014) on protective measures in a nuclear or radiological accident, early  
 246 protective actions such as evacuation, sheltering and partial sheltering are only justified if the  
 247 projected dose is above 20 mSv the first week, above 10 mSv over two days and 1-10 mSv in  
 248 two days, respectively. Countermeasures to reduce external and inhalation doses are thus not  
 249 justified in this scenario and this exposure pathway was not investigated further.

250



252 Figure 4: Total effective dose from inhalation and external exposures of  $^{137}\text{Cs}$  after one week (left), one month (middle) and  
 253 one year (right) calculated by ARGOS. Blue:  $< 0.01$  mSv, pink:  $0.01 - 0.1$  mSv, Purple:  $> 0.1$  mSv.

### 254 3.3 Food chain modelling

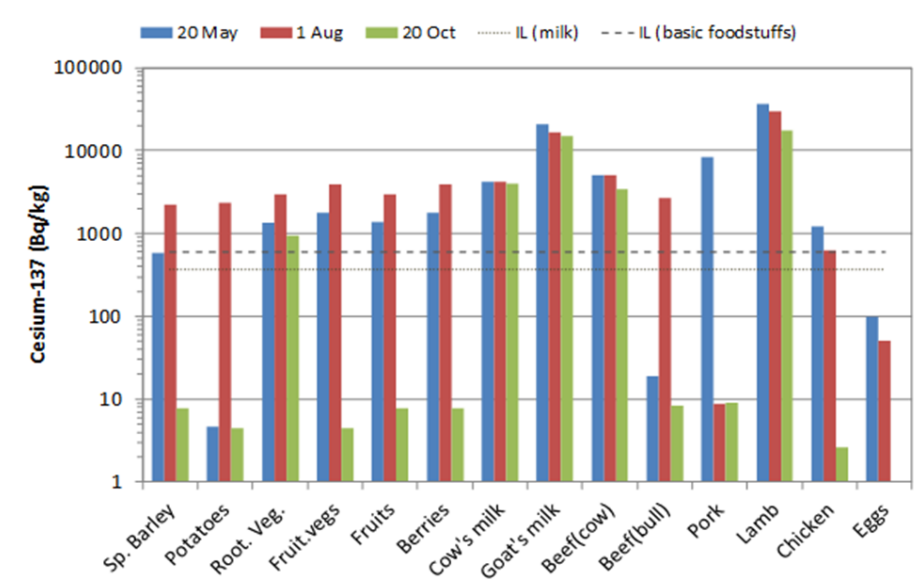
#### 255 3.3.1 Agricultural produce - FDMT

256 The model was run for Vindafjord municipality where the predicted deposition was  
 257  $130 \text{ kBq m}^{-2}$  of  $^{137}\text{Cs}$  for our hypothetical scenario. The default values in FDMT were used  
 258 (Müller et al, 2004) (see Appendix A.1.3 for details). FDMT generally assumes all fodder to  
 259 be locally produced, including feed concentrates. Pigs, poultry and cattle (bulls) are not  
 260 presumed to be on pasture, so contamination of products from such animals is mainly due to  
 261  $^{137}\text{Cs}$  levels in the concentrates. Note that concentrates in Norway are usually not locally  
 262 produced, so it can be debated whether it is justified to include model results for such  
 263 products. We have, however, kept them based on an argument of being “conservative”.

264 Since agricultural impacts vary considerably with deposition time of the year, we  
 265 chose to run the scenario with three deposition dates: 20 May, 1 August and 20 October.  
 266 Figure 5 shows the highest estimated concentrations with FDMT for the three deposition  
 267 dates. With a deposition on 20 May, all foodstuffs except potatoes, beef (cattle) and eggs are  
 268 predicted to exceed the Norwegian food intervention levels of  $370 \text{ Bq kg}^{-1}$  for milk and infant  
 269 foods and  $600 \text{ Bq kg}^{-1}$  for all other basic foodstuffs. For a deposition on 1 August, all

270 foodstuffs except pork and eggs are predicted to exceed the limits. For a deposition on 20  
 271 October, on the other hand, only root vegetables, cow`s milk, goat`s milk, beef (cows) and  
 272 lamb meat would exceed the limits.

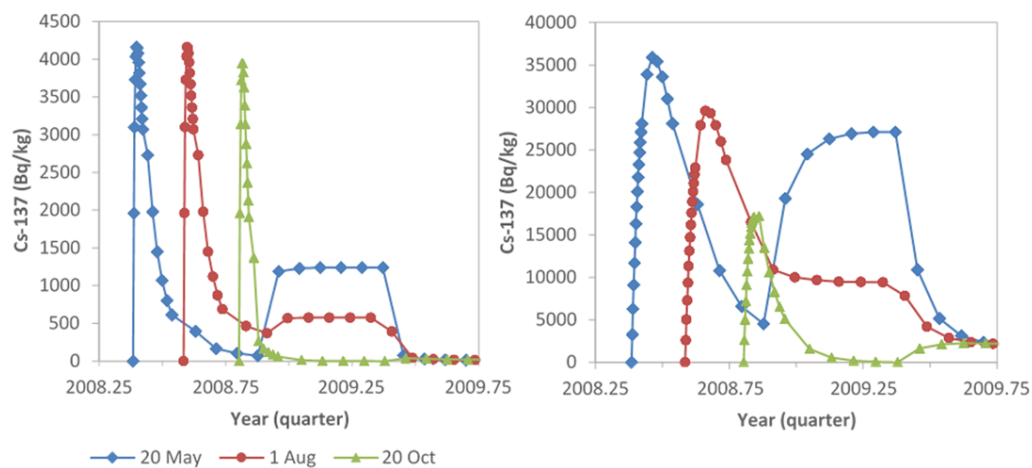
273 The time development of concentrations in cow`s milk and lamb meat is shown in  
 274 Figure 6. The predicted concentrations are significantly higher in lamb meat than in cow`s  
 275 milk and the concentrations remain well above the food intervention level in meat even for  
 276 the second year. The second peak observed for the red and blue lines is due to feeding with  
 277 hay contaminated by the event, then cut and stored for later use. Without any mitigating  
 278 actions the concentration in lamb meat from Vindafjord is predicted to be  $> 600 \text{ Bq kg}^{-1}$  for  
 279 10–20 years due to extensive grazing.



280  
 281 *Figure 5: Highest estimated concentrations of  $^{137}\text{Cs}$  ( $\text{Bq kg}^{-1}$ ) in various foodstuffs predicted for the five year period using*  
 282 *FDMT for three deposition dates: 20 May (blue), 1 August (red) and 20 October (green). The food intervention level for*  
 283 *milk, IL (milk), and for other basic foodstuffs, IL (basic foodstuffs), are shown with dotted lines.*

284 If we assume that all consumed food is locally produced, the internal doses from a  
 285 contaminated diet in Vindafjord municipality would be up to 9.1 mSv for adults and 3.8 -7.0

286 mSv for children in Rogaland over 5 years if no agricultural countermeasures were  
 287 implemented (Table 2). The largest part of the dose is received during the first year. It thus  
 288 exceeds the general Norwegian recommendation to keep total radiation doses to the public  
 289 from radioactive contamination below 1 mSv/y and also the Nordic guidelines and  
 290 recommendations (2014) which state that the aim is to keep ingestion doses below 1 mSv/y  
 291 the first year after an accident.



292  
 293 *Figure 6: Time development of concentrations ( $Bq\ kg^{-1}$ ) in cow's milk (left) and lamb meat (right) for Vindafjord*  
 294 *municipality with a deposition of  $130\ kBq/m^2$  of  $^{137}Cs$  on three different dates – 20 May (blue), 1 August (red) and 20*  
 295 *October (green). Please note the different scales on the y-axes for the two figures.*

296 *Table 2: Ingestion doses from  $^{137}Cs$  (mSv) for different age groups calculated by FDMT for the Vindafjord municipality*  
 297 *where the modelled deposition was  $130\ kBq\ m^{-2}$ .*

Individual ingestion doses (mSv) from Cs-137		
Age (y)	First year	After 5 years
1	4,7	4,8
5	3,3	3,6
10	4,2	4,6
15	6,4	7,0
Adults	8,3	9,1

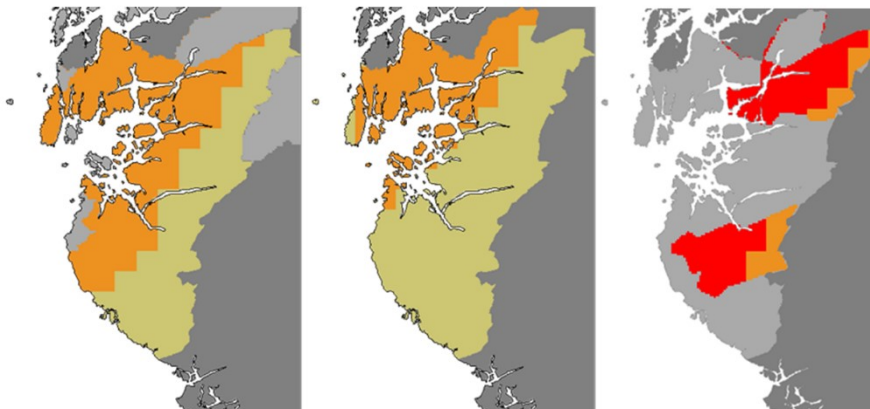
298  
 299 **3.3.2 Rough grazing animal products and wild foodstuffs - STRATOS**  
 300 The deposition map was combined with three aggregated transfer factors ( $T_{ag}$ 's) (expected,  
 301 min, max) (see Appendix A.1.4 for details) for rough grazing animal products and wild



302 foodstuffs. The modelled concentrations were compared to the food intervention levels for  
303  $^{137}\text{Cs}$  for trade of  $600 \text{ Bq kg}^{-1}$  for mushrooms, berries, and cheese;  $370 \text{ Bq kg}^{-1}$  for milk; and  
304  $3000 \text{ Bq kg}^{-1}$  for game. As examples, the resulting maps presented in Figure 7 show which  
305 areas are expected to show activity concentrations above these limits for roedeer, wild berries  
306 and brown whey goat cheese.

307 The modelled concentrations can be combined with the statistics for production and  
308 hunting to show how large percentage of the annual production/yield will be above the food  
309 intervention level. For instance, 56 % of the produced goat's milk in Rogaland was estimated  
310 to be above the intervention level for milk.

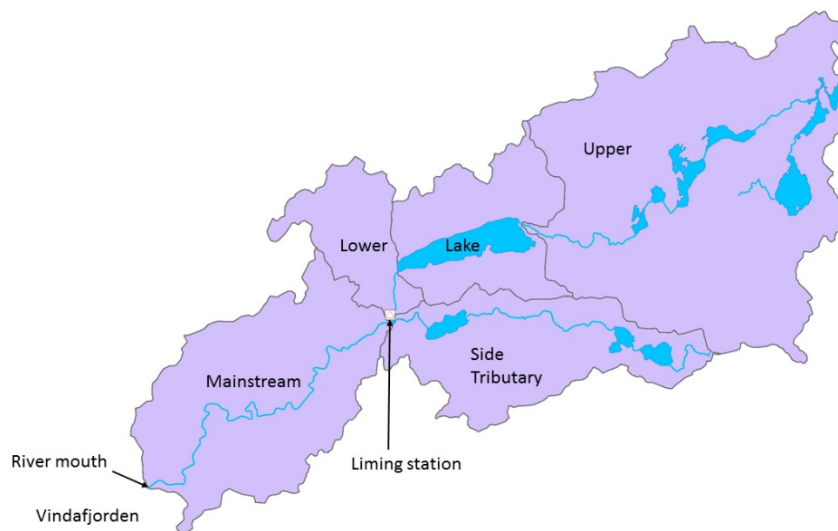
311 This model can be used for any wild foodstuff or rough grazing animal as long as  
312 three  $T_{ag}$ 's (expected, min, max) can be properly estimated and the geographical distribution  
313 of production/hunting/gathering is known from e.g., regional or national statistics. The  
314 predicted concentrations can be further used in the ERICA Tool to calculate dose rates to  
315 terrestrial animals and plants.



316  
317 *Figure 7: Maps indicating where food intervention levels might be exceeded for roedeer (left), wild berries (middle) and*  
318 *brown whey goat cheese (right). Colour coding: Red (lowest  $T_{ag}$ ) – product will clearly be above in the long term*  
319 *perspective – years to decades; orange (expected  $T_{ag}$ ) - product will most probably be above in the long term perspective*  
320 *(years); kaki (highest  $T_{ag}$ ) – product might be above in the first year, but probably not in the following years; light grey – no*  
321 *production or hunting in this area; dark grey – outside Rogaland County.*

### 322 3.4 Freshwater modelling - INCA-RAD

323 The Vikedal area consists of various lakes, streams and catchment areas with a main  
324 river that flows into the fjord Vindafjorden, an arm of the fjord Boknafjorden. The river  
325 Vikedal is popular for salmon fishing. The area has a coastal climate and the river may  
326 experience high flows particularly in the autumn. The map in Figure 8 shows the five  
327 different sub-catchments of the Vikedal catchment that are used in the modelling  
328 calculations. As an acid rain countermeasure, the lower part of Vikedal River has been  
329 extensively limed since 1987 (Sandlund et al., 2010). Due to a physical barrier (the liming  
330 station), the salmon and sea trout cannot migrate beyond the main river.



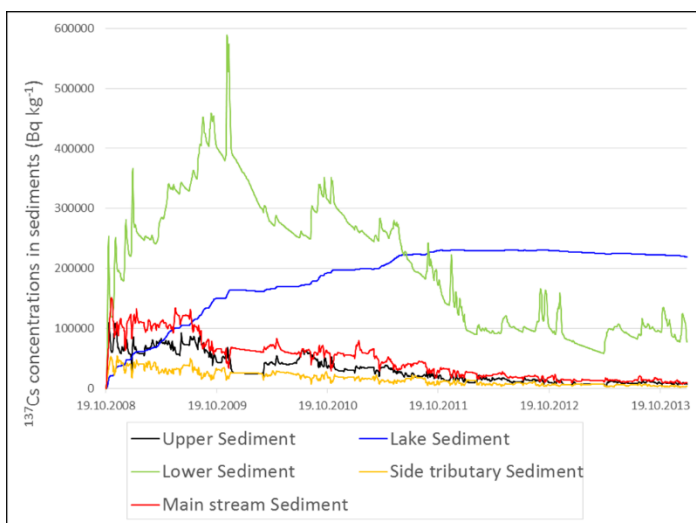
331  
332 *Figure 8: Map over the Vikedal catchment with a division into five sub-catchments used in the calculations: Upper, Lake,*  
333 *Side Tributary, Lower and Main stream. The liming station in the Vikedal River and the river mouth is indicated with*  
334 *arrows.*

335 A mean geometric value for  $K_d$  of  $2.9 \cdot 10^4$  L/kg (IAEA, 2010), was selected to run the  
336 INCA-RAD model for  $^{137}\text{Cs}$  for the time period 19.10.2008 to 14.01.2014 using monitoring  
337 data for water flow from the Norwegian Water Resources and Energy Directorate and the  
338 SNAP raster files for deposition of  $^{137}\text{Cs}$  ( $\text{Bq m}^{-2}$ ). The results were activity concentrations in  
339 both water ( $\text{Bq m}^{-3}$ ) and sediments ( $\text{Bq kg}^{-1}$ ) in the five different sub-catchments in daily time  
340 steps. The predicted concentrations in water were fluctuating according to the daily water

341 flow and generally decreasing steadily over time. The predicted concentrations in water were  
 342  $<10 \text{ Bq l}^{-1}$  for  $^{137}\text{Cs}$  for all areas, decreasing over time to a few  $\text{Bq l}^{-1}$  or less. For sediments,  
 343 however, substantial concentrations were predicted, in particular in the Lake and Lower areas  
 344 reaching levels of 223 000 and 574 000  $\text{Bq kg}^{-1}$ , respectively, while the sediment  
 345 concentrations peaked around 150 000  $\text{Bq kg}^{-1}$  in the Main stream. In all sub-catchments but  
 346 the Lake, the sediment concentrations are decreasing with time over the five years (see Figure  
 347 9).

348 INCA-RAD also predicted the outflow of  $^{137}\text{Cs}$  to the estuary in Vindafjord in  $\text{Bq d}^{-1}$   
 349 for the same time period. The size of the drainage area and the deposition of radioactivity  
 350 within the Vikedal area was used to estimate monthly outflow to the sea from 21 main rivers  
 351 in Norway. They were used as additional point sources with a time-dependent flux of  $^{137}\text{Cs}$   
 352 into the marine ocean model ROMS (see section 3.6.1).

353



354

355 *Figure 9: Time development of  $^{137}\text{Cs}$  concentrations in sediments ( $\text{Bq kg}^{-1}$ ) for all five areas.*

### 356 **3.5 Dose rates to aquatic organisms: from INCA-RAD to the ERICA Tool**

357 The data on  $^{137}\text{Cs}$  in water and sediments from INCA-RAD were used as input to the  
 358 ERICA Tool version 1.0 to calculate dose rates to native biota. The report from Sandlund et  
 359 al. (2010) gives an overview of the aquatic species present in the Vikedal area. They are

360 presented in Table 3 together with the corresponding ERICA reference organisms and the  
 361 concentration ratios and occupancy times used. Occupancy times are important in calculating  
 362 dose rates since the exposures are either coming only from the contaminated water (for  
 363 pelagic fish, salmon, zooplankton), only from the contaminated sediments (for insect larvae  
 364 that live within the sediments) or from both water and sediments for gastropods and  
 365 crustaceans that live on the sediment surface.

366

367 *Table 3: Reference organisms and parameter values used in the ERICA Tool calculations*

<b>ERICA reference organism</b>	<b>Representative species present in Vikedal</b>	<b>Concentration ratios</b> <i>Derived from</i>	<b>Occupancy times</b>
Pelagic fish	brown trout ( <i>Salmo trutta</i> ) and Arctic char ( <i>Salvelinus alpinus</i> )	7100 L/kg <i>ERICA default value</i>	100 % in water
Salmon	Atlantic salmon ( <i>Salmo salar</i> ) and sea trout ( <i>Salmo trutta trutta</i> )	5600 L/kg <i>Hosseini et al, 2008</i>	100 % in water
Crustacean	various copepod species e.g. <i>Eudiaptomus gracilis</i>	$1.04 \cdot 10^4$ L/kg <i>ERICA default value</i>	100 % on sediment surface
Gastropod	freshwater snails e.g. <i>Lymnaea peregra</i> , <i>Radix balthica</i>	2800 L/kg <i>ERICA default value</i>	100 % on sediment surface
Insect larvae	larvae of mayfly such as <i>Baetis rhodani</i>	$1.04 \cdot 10^4$ L/kg <i>ERICA similar reference organism extrapolation</i>	100 % in sediments
Zoo-plankton	various species	1560 L/kg <i>ERICA default value</i>	100 % in water

368

369 The ERICA Tool has not yet incorporated a kinetic approach to uptake and depuration  
 370 in organisms. Thus, daily fluctuations in dose rates according to daily variations in the

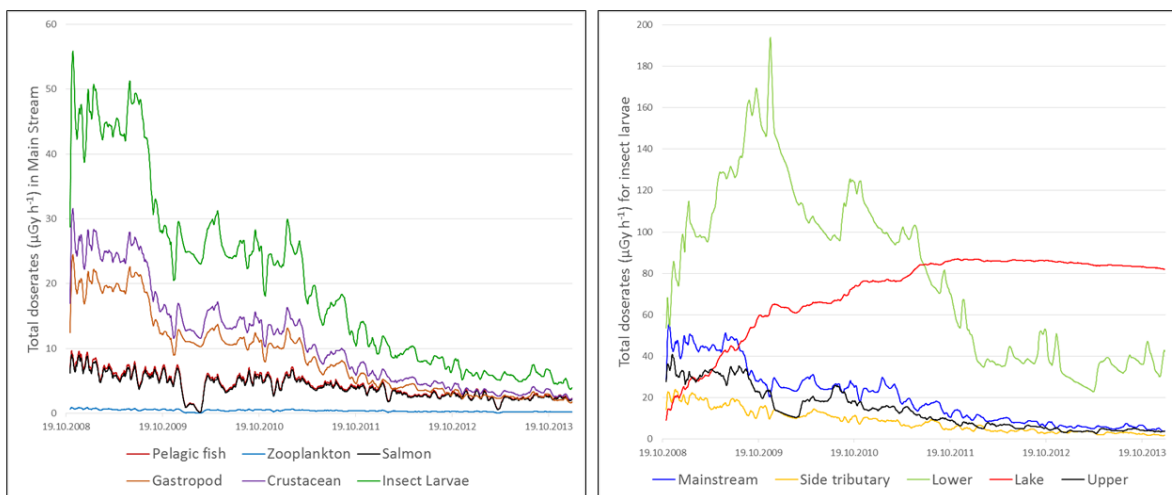
371 concentrations in water and sediment, would not be representative of real life. A moving  
372 average over 15 days has been applied to the data on dose rates to account for this limitation.

373 The results from the combination of INCA-RAD and the ERICA Tool for six  
374 reference organisms in the Main Stream are shown in Figure 10 (left). The dose rates for  
375 pelagic species reflects the flow pattern and the development in water concentrations over  
376 time. Time periods of low flow, for instance, would be reflected in a dip in predicted dose  
377 rates to pelagic species (Figure 10, left). The dose rates for sediment dwelling organisms are  
378 related to the slower sedimentation processes with a large variation in predicted sediment  
379 concentrations between the five different areas (Figure 9).

380 The dose rates to zooplankton were very low, resting below  $2 \mu\text{Gy h}^{-1}$  for the whole  
381 period in all areas. The dose rates to salmon and pelagic fish were very similar and reached  
382 levels of around  $10\text{-}12 \mu\text{Gy h}^{-1}$  after a few days, then steadily decreased with time to levels  
383 below  $2 \mu\text{Gy h}^{-1}$  after a few years. The dose rates were clearly higher for sediment dwelling  
384 organisms than pelagic ones as shown for the Main Stream (Figure 10, left). This was  
385 predicted for all five areas (not shown). The dose rates are highest for insect larvae due to an  
386 anticipated 100 % occupancy time within the sediments. Due to sedimentation processes, the  
387 time development was very different in the Lake and in the Lower area compared to the other  
388 areas, as shown for insect larvae (Figure 10, right). For the Lake the dose rates increased for  
389 the first three years and then decreased very slowly. The dose rates after five years were  
390 around 35, 40 and  $80 \mu\text{Gy h}^{-1}$  for gastropods, crustaceans and insect larvae, respectively. In  
391 the Lower area the dose rates increased steadily for the first year to around  $100 \mu\text{Gy h}^{-1}$  for  
392 gastropods,  $110 \mu\text{Gy h}^{-1}$  for crustaceans and  $220 \mu\text{Gy h}^{-1}$  for insect larvae, then steadily  
393 decreased over the following years. For sediment dwelling organisms the exposure was  
394 significantly higher than the ERICA screening value of  $10 \mu\text{Gy h}^{-1}$  indicating that a more  
395 detailed site-specific study would be needed (in the event of an accident) to address the

396 potential environmental risk. The modelled dose rates for sediment dwelling organisms are  
397 very sensitive to the modelled sediment concentrations, which in turn strongly depends on the  
398 sediment particulate matter value used in INCA-RAD.

399 Although the dose rates in pelagic fish remain low, the corresponding predicted  
400 concentrations in brown trout and Arctic char peaked at values around 58 500 Bq kg<sup>-1</sup> in the  
401 Lake after 16 days. The values for salmon and sea trout in the Main Stream peaked at 51 000  
402 Bq kg<sup>-1</sup>. After 5 years the predicted concentrations had decreased to around 4500 Bq kg<sup>-1</sup> for  
403 brown trout and Arctic char in the lake while for salmon and sea trout they had decreased to  
404 around 3500 Bq kg<sup>-1</sup> in the Main Stream. Although the dose rates hardly exceeded the  
405 ERICA screening value of 10 µGy h<sup>-1</sup> (Brown et al., 2008) indicating negligible  
406 environmental risk, the concentrations predicted in these fish species were clearly much  
407 higher than the food intervention level for wild freshwater fish in Norway which is currently  
408 3000 Bq kg<sup>-1</sup> for <sup>137</sup>Cs if traded for human consumption.

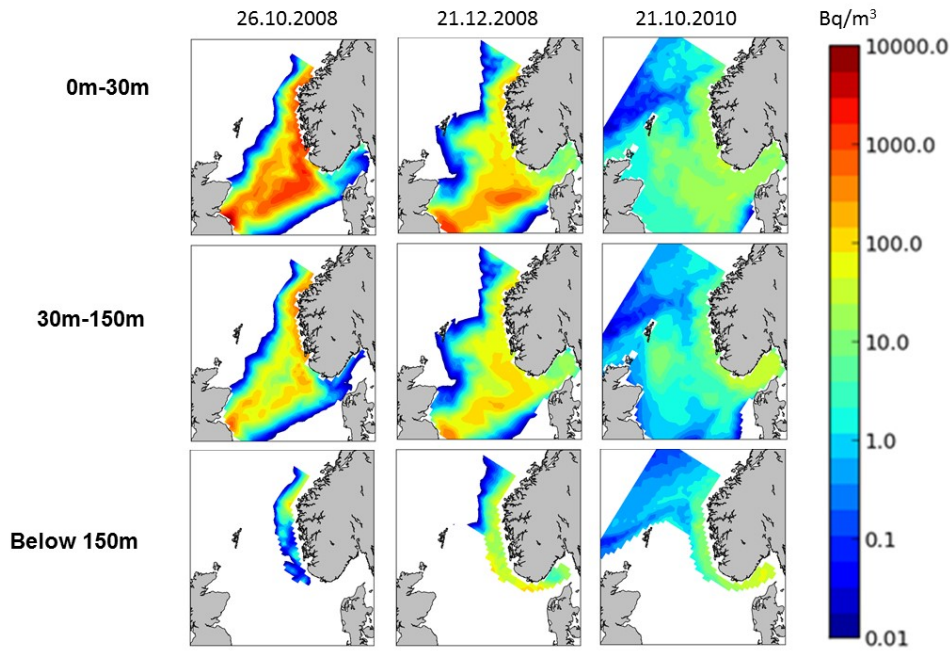


409  
410 *Figure 10: Dose rates (µGy h<sup>-1</sup>) from <sup>137</sup>Cs for six reference organisms calculated with the ERICA Tool for the Main stream*  
411 *(left). Compared dose rates for insect larvae (right) from the five areas. All data transformed with a moving average of 15*  
412 *days. Please note the different scale on the two y-axes.*

## 413 **3.6 Marine modelling**

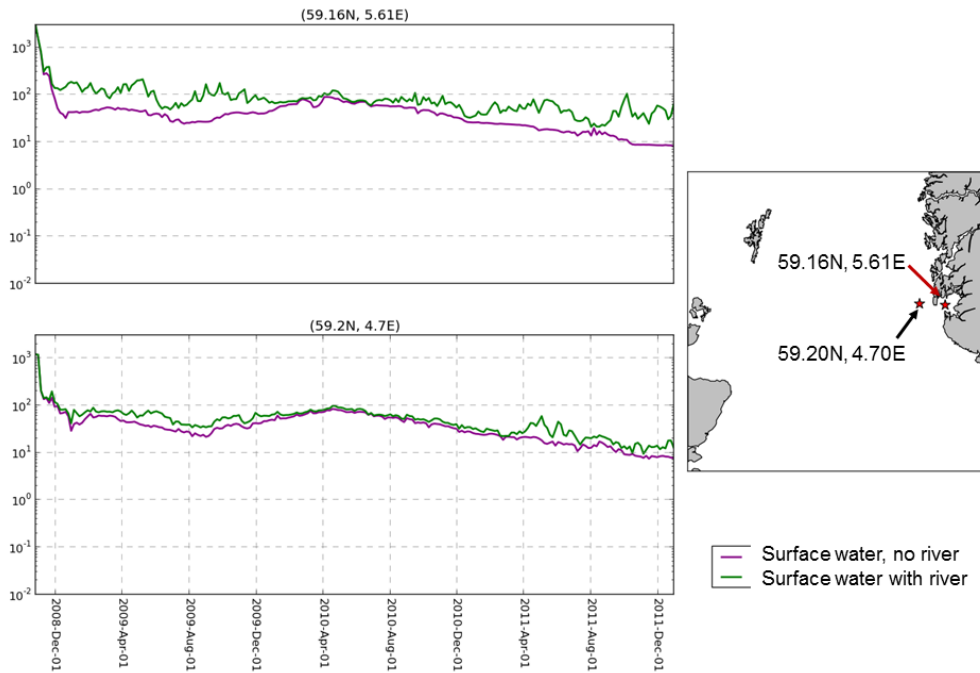
### 414 **3.6.1 ROMS**

415 The results from the dispersion modelling for three water depths at different dates  
416 after deposition are shown in Figure 11. For any chosen point in coastal areas or offshore, the  
417 variation in concentrations over time can be shown as a transect time series. This is shown in  
418 Figure 12 for two locations. The simulations were done both with and without riverine input  
419 as additional point sources. The magnitude of the riverine input was more pronounced closer  
420 to the Vikedal river mouth, i.e., in Boknafjorden, than in open waters off the coast. These  
421 data can be used to calculate concentrations in pelagic marine organisms and corresponding  
422 dose rates with the ERICA Tool as done for freshwater species. In Boknafjorden, when the  
423 outflow from the Vikedal River is taken into account, the predicted peak  $^{137}\text{Cs}$  activity  
424 concentrations (using the ERICA Tool version 1.2) were up to  $257 \text{ Bq kg}^{-1}$  in pelagic fish, in  
425 macroalgae  $294 \text{ Bq kg}^{-1}$  and in molluscs  $153 \text{ Bq kg}^{-1}$  six days after deposition, decreasing  
426 rapidly to  $< 20 \text{ Bq kg}^{-1}$  for all categories after one month. The corresponding peak dose rates  
427 were  $4.7$  (pelagic fish),  $5.4$  (macroalgae) and  $5.2$  (mollusc)  $\mu\text{Gy h}^{-1}$ . Default values from the  
428 ERICA Tool version 1.2 were used for all calculations.



429

430 Figure 11: The dispersion calculated by ROMS for  $^{137}\text{Cs}$  concentration ( $\text{Bq m}^{-3}$ ) at three water depths: 0-30 m (top row), 30-  
 431 150 m (middle row), below 150 m (bottom row) – and at three different dates after deposition: 26 October 2008 (left  
 432 column), 21 December 2008 (middle column), 21 October 2010 (right column).



433

434 Figure 12: Transect concentrations for  $^{137}\text{Cs}$  ( $\text{Bq m}^{-3}$ ) in Boknafjorden (59.16N, 5.61E) (top) and  
 435 off the coast (59.20N, 4.70E) (bottom) in surface water (0-30 m) without riverine input in purple. Green lines show the concentrations when  
 436 riverine input is included in the model runs.



### 437 **3.6.2 NRPA marine box model**

438 The deposition on surface ocean water ( $\text{Bq m}^{-2}$ ) was aggregated into total deposition  
439 per box and then used as input to the model with a deposition date of 20 October 2008. The  
440 total deposition in the box closest to Rogaland was assumed to be  $3.25 \cdot 10^{15}$  Bq of  $^{137}\text{Cs}$ . The  
441 model presumes that the radionuclides are instantaneously and uniformly mixed within the  
442 box. The radionuclides are then dispersed through the boxes and compartments with time.  
443 The concentration ratio values used were  $100 \text{ L kg}^{-1}$  for pelagic fish, 50 for crustaceans and  
444 66 for molluscs according to IAEA (2004). The modelled concentrations were below  $40 \text{ Bq}$   
445  $\text{kg}^{-1}$  for all three species shortly after the accident, rapidly decreasing to  $< 5 \text{ Bq kg}^{-1}$  within a  
446 few months. The corresponding dose rates predicted by the NRPA box model for the same  
447 organisms were all below  $0.2 \mu\text{Gy h}^{-1}$ .

### 448 **3.6.3 Comparison of ROMS and NRPA box model results**

449 The modelled concentrations and dose rates obtained by the dynamic ROMS model  
450 and by the NRPA box model have been compared, considering that only the former includes  
451 riverine input and dynamic dispersion. The ERICA Tool, using input from ROMS on water  
452 contamination, predicted concentrations about 7 times higher for pelagic fish in Boknafjorden  
453 than the NRPA box model for the box closest to Rogaland. However, water concentrations  
454 modelled by ROMS for the ocean area off the coast were about five times lower than within  
455 the fjord Boknafjorden closer to the river outlet (Figure 12). The concept of instantaneous  
456 and uniform mixing within the NRPA box model implies that the activity concentrations in  
457 the box closest to Rogaland should be more comparable to the ROMS area off the coast.  
458 Indeed, the modelled concentrations in fish is in relatively good agreement (differing with a  
459 factor of  $< 2$ ) for the ocean areas off the coast of Boknafjorden.

### 460 ***3.7 Comparison with post-Chernobyl data***

461 It is clear that an accident with an atmospheric release of this magnitude could  
462 potentially contaminate large areas substantially. The modelled deposition using a real  
463 historical weather scenario predicted deposition levels in Norway comparable to the  
464 Chernobyl accident (Figure 3). From experience, we know that this would lead to decades of  
465 challenges; over 30 years after the Chernobyl fallout event, countermeasures are still  
466 implemented in Norway to reduce the levels of  $^{137}\text{Cs}$  in milk and meat to comply with the  
467 Norwegian food intervention levels for trade (Komperød et al., 2017) . A fallout of this  
468 magnitude would require decades of monitoring and countermeasures.

469 The predicted inhalation and external doses to humans were low and early protective  
470 actions such as evacuation or sheltering would not have been justified according to the  
471 Nordic guidelines and recommendations (2014) for protective measures in nuclear or  
472 radiological emergency. This is mainly due to the absence of short-lived radionuclides in the  
473 present scenario, which are usually contributing substantially to inhalation and external doses  
474 (e.g.,  $^{131}\text{I}$ ,  $^{134}\text{Cs}$ ,  $^{133}\text{Xe}$ ,  $^{132}\text{Te}$ ).

475 The internal doses through a contaminated agricultural diet, however, would exceed  
476 the recommended maximum level of 1 mSv/y from ingestion. The predicted activity  
477 concentrations in agricultural produce were above maximum permitted levels and comparable  
478 to  $^{137}\text{Cs}$  levels measured in Norway after the Chernobyl accident: i.e., up to 40 000 Bq kg<sup>-1</sup> in  
479 lamb meat, 1200 Bq l<sup>-1</sup> in cow`s milk and 2900 Bq l<sup>-1</sup> in goat`s milk (Liland and Skuterud,  
480 2013). Agricultural countermeasures are clearly justified in this situation.

481 The predicted concentrations in freshwater fish are comparable to post-Chernobyl  
482 values as well, around 35 000 Bq kg<sup>-1</sup> of  $^{137}\text{Cs}$  was reported by Strand et al. (1992) and  
483 Brittain and Gjerset (2010) for pelagic fish in Norwegian lakes. Also other forest foodstuffs  
484 such as mushrooms, berries and game were predicted to exceed the food intervention levels

485 for trade the first years in some areas, which was also the case after the Chernobyl accident  
486 (Liland and Skuterud, 2013).

487 The contamination of marine species by  $^{137}\text{Cs}$  was low after the Chernobyl accident,  
488 up to a few tens of Bq/kg in fish (IFE, 1986) since the deposition was very low in Norwegian  
489 marine areas. For this hypothetical scenario, we cannot rule out that food intervention levels  
490 might be exceeded for seafood close to the Vikedal river outlet (or other river outlets on the  
491 western coast) shortly after the accident. However, the transfer of  $^{137}\text{Cs}$  to organisms in sea  
492 water is much lower than in freshwater so in general activity concentrations in marine fish  
493 and other seafood (wild and farmed) are predicted to stay below Norwegian food intervention  
494 levels. At the same time, the seafood market is very sensitive to information or rumours about  
495 contamination, and the export from Norway might be negatively affected even with low  
496 contamination levels due to public and market fear of radioactive contamination.

497 It should be noted that we have here compared true measurement data after the  
498 Chernobyl accident with conservative model estimates for a hypothetical accident. They are  
499 thus not directly comparable, but the model estimates are in the same order of magnitude as  
500 the measured data. This indicates that the model estimates are reasonable.

501 Furthermore, it should be noted that only  $^{137}\text{Cs}$  was included in the pilot study  
502 described, although the HAL contains other long-lived radionuclides, too (see Appendix 2).  
503 Of these,  $^{90}\text{Sr}$  would be present in large quantities and has a known high transfer in terrestrial  
504 food chains. This would add to the challenges presented for  $^{137}\text{Cs}$ .

505

### 506 ***3.8 Key factors contributing to uncertainty***

507 At the time this study was performed, the models did not have built-in uncertainty  
508 ranges when stating the results, although there are known variabilities and uncertainties in all  
509 of them. A single value, deterministic output from one model was used as input to the next

510 model and this procedure was repeated along the whole chain of models. Each model was  
511 used to give a best estimate result, and no account was taken of the various inherent  
512 uncertainties associated with the calculations such as input, interpolation and extrapolation  
513 uncertainty, parameter uncertainty and variability, and algorithmic or structural uncertainty  
514 (Salbu, 2016). It is challenging to ascertain whether the results from the modelling chain can  
515 be deemed accurate or truly representative of the environmental system. The comparison  
516 between the modelled activity concentrations for the Sellafield scenario and the post-  
517 Chernobyl monitoring data on <sup>137</sup>Cs in Norway indicates, however, that the predicted values  
518 are within a realistic range.

519         Investigations have earlier been performed to identify the key factors contributing to  
520 uncertainties within each model, such as sensitivity analyses and expert judgements (e.g.,  
521 Sørensen et al. (2014); Vives i Batlle et al. (2008); Iosjpe (2011); Iosjpe and Liland (2012);  
522 Iosjpe and Logemann (2014); Avila et al. (2004); Hansen et al. (2010)). Since one of the  
523 main CERAD goals is to reduce uncertainties in risk and impact assessments, further work  
524 has already been undertaken or is ongoing within CERAD to address this. Reducing the  
525 uncertainties in the models used in this pilot study is not only a question of finding the best  
526 parameter values and their underlying statistics/distributions; it is also important that the  
527 underlying model uses the most realistic representation of the geographical area and  
528 ecosystem studied.

529         Table 4 lists the key factors contributing to uncertainty for each model. Some of these  
530 key factors were prioritized in 2016 for updating through CERAD research (see Table 4, last  
531 column), based on their magnitude and the feasibility of reducing their influence on the total  
532 uncertainty in model calculations. Work to reduce these uncertainties continues to be a  
533 priority of CERAD, but is too extensive to be fully described here. Some of the work already  
534 undertaken since this study was performed, is presented below with due references.

Table 4: Key factors contributing to uncertainty for each model and those prioritized for updating in CERAD

Model	Key factors contributing to uncertainty	Prioritized updating in CERAD
<b>SNAP</b>	<ol style="list-style-type: none"> <li>1. Model formulation</li> <li>2. Input data <ul style="list-style-type: none"> <li>– Inaccurate or wrong source term description (<i>location; time; particle size, density, shape; release rates and vertical range</i>)</li> <li>– inaccurate or missing meteorological input data (<i>precipitation field, velocity field, temperature field</i>)</li> <li>– Incomplete or over-simplified parametrizations in the model (<i>wet and dry deposition, advection and diffusion</i>)</li> </ul> </li> </ol>	<ul style="list-style-type: none"> <li>• Use ensemble meteorological prediction instead of deterministic predictions</li> <li>• Improve parametrization of: <ul style="list-style-type: none"> <li>– wet deposition (particle size/ density, precipitation) type/form/vertical distribution</li> <li>– dry deposition (particle shapes, receptor conditions)</li> </ul> </li> </ul>
<b>ARGOS DSS</b>	<ol style="list-style-type: none"> <li>1. For human dose assessments: <ul style="list-style-type: none"> <li>– particle sizes, breathing rate, occupancy and shielding effects from houses</li> </ul> </li> </ol>	<ul style="list-style-type: none"> <li>• Particle sizes, will be done as part of SNAP</li> </ul>
<b>FDMT</b>	<ol style="list-style-type: none"> <li>1. Default data representative of Southern Germany: <ul style="list-style-type: none"> <li>– Growth periods, leaf area indices, crop yields, migration rates</li> <li>– Transfer factors (TF), animal specific feeding rations, period of preparing winter feed</li> <li>– Human age-dependent consumption rates, seasonality of consumption rates</li> </ul> </li> </ol>	<ul style="list-style-type: none"> <li>• Regional updating to Norwegian parameter values for: <ul style="list-style-type: none"> <li>– growing season, harvest periods</li> <li>– feeding rations of cows, goats and lamb/sheep</li> <li>– <sup>137</sup>Cs and <sup>90</sup>Sr transfer factors for milk and meat</li> <li>– human age-dependent diets</li> </ul> </li> </ul>
<b>STRATOS</b>	<ol style="list-style-type: none"> <li>1. Deposition</li> <li>2. Aggregated transfer factors (<math>T_{ag}</math>'s)</li> <li>3. Production/hunting/gathering statistics</li> </ol>	<ul style="list-style-type: none"> <li>• Fieldwork to establish regional <math>T_{ag}</math>'s</li> <li>• Extension to include <sup>90</sup>Sr</li> </ul>
<b>INCA-RAD</b>	<p>In order of relative importance for final sensitivity:</p> <ol style="list-style-type: none"> <li>1. Sediment transport (<i>entrainment rate, splash erosion rate, flow erosion rate</i>)</li> <li>2. Mineralization rate of solid organic matter</li> <li>3. <math>K_d</math></li> <li>4. Residence time of water in the organic layer</li> <li>5. Rate of solid organic matter to dissolved organic matter</li> </ol>	<ul style="list-style-type: none"> <li>• Sediment transport</li> <li>• <math>K_d</math> (<i>distribution coefficient between particle and water phase</i>)</li> <li>• <math>K_{w-doc}</math> (<i>partitioning coefficient between water and dissolved organic carbon</i>)</li> <li>• Speciation codes</li> <li>• Transformation processes</li> </ul>

	6. $K_{w-doc}$ 7. Temperature correction constant 8. Hydrological parameter for calculating the velocity of flow	
<b>ROMS</b>	1. Ocean model dynamics ( <i>initial or boundary conditions, model resolution, description of turbulent mixing</i> ) 2. Particle processes not included ( <i>assumes passive, non-interacting radionuclides</i> ) 3. Missing description of mixing zones in estuaries	<ul style="list-style-type: none"> <li>• Increase resolution</li> <li>• Include radionuclide particle interactions</li> <li>• Include chemical speciation, particle sizes and kinetics of transformation processes, in particular for estuaries</li> </ul>
<b>NRPA box model</b>	For $^{137}\text{Cs}$ in the Norwegian Current: 1. Porosity 2. Sediment distribution coefficient ( $K_d$ ) 3. Reworking rate 4. Concentration factor (CF)  <i>(For other radionuclides also: suspended sediment load, sedimentation rate, and coefficient of molecular diffusion)</i>	<ul style="list-style-type: none"> <li>• For dispersion in water and sediments: porosity, <math>K_d</math>, sedimentation rate, suspended sediment load, coefficient of molecular diffusion</li> <li>• For bioaccumulation: CF, assimilation efficiency for different trophic levels, ingestion and excretion rates</li> <li>• Include biokinetics</li> </ul>
<b>ERICA Tool</b>	1. Assumes equilibrium conditions 2. Concentration ratios 3. $K_d$ 4. Bioavailability and mobility of radionuclides in the environment 5. Bioaccumulation factors 6. Gut uptake fraction	<ul style="list-style-type: none"> <li>• Develop dynamic approach</li> <li>• Include biokinetics</li> <li>• Characterize time-dependent uptake, assimilation and depuration of radionuclides</li> </ul>

536  
537

The main sources of uncertainty for the SNAP model are the model formulation

538 including the conceptual understanding of the source term, and in the parametrization of the  
 539 input data. Uncertainties in the model formulation are related to our incomplete knowledge of  
 540 the physical processes responsible for atmospheric transport and deposition of radioactive  
 541 debris. In all severe nuclear accidents, radioactive particles ranging from submicrons to  
 542 fragments will be released (IAEA, 2011; Salbu 2016). Particulate fallout would result in non-  
 543 homogeneous hot-spots and single particles could become internal point sources if inhaled or  
 544 ingested by humans or animals (Ytre-Eide et al., 2009), but this was not taken into account in  
 545 our present study. If particles are present in the release, the size and density would influence

546 the particle transport pattern and the deposition map as well as the subsequent ecosystem  
547 transfer estimates, being quite different from that of aerosols. If particles are ignored, the  
548 conceptual uncertainty in the source term is high.

549 Another example of source term uncertainty is the timing of an event. In this case  
550 study, MET Norway showed that a 3 hours difference in start time of the accident gives  
551 concentration and deposition changes with a factor of four. Likewise, uncertainty related to  
552 parametrization of wet deposition (due to variations in particle size and density, precipitation  
553 amount) in the present model structure is estimated to  $\pm 50\%$  while for advection and  
554 diffusion it is estimated to only  $\pm 20\%$ .

555 Regarding FDMT, the model outcomes are highly sensitive to the deposition time and  
556 to variations in a number of other input parameters. These parameter sensitivities are case  
557 specific (Müller and Pröhl, 1993), and does not provide general answers regarding the model  
558 uncertainties. However, general recommendations are available within the RODOS or  
559 ARGOS communities in relation to regional updating – where different parameters have been  
560 rated as being of high, moderate or low priority by the developers of ECOSYS or other  
561 experienced users of FDMT (Pröhl and Müller, 2005); (Raskob et al., 2000); (Hansen et al.,  
562 2010). Our priority parameters shown in Table 4 are largely based on these expert judgement  
563 recommendations. Important parameters in relation to adaptation to Nordic conditions have  
564 recently been identified and updated (Thørring et al., 2016) – focusing on (1) parameters of  
565 relevance to growing season and harvest periods of crops and grass, including seasonal  
566 development of leaf area indices (LAI), (2) animal feeding practice, and (3) human  
567 consumption of foodstuffs. Regional adaptation continues with work initiated on e.g., transfer  
568 and time-development of relevant radioelements. Furthermore, probabilistic simulations in  
569 FDMT is presently under development, as opposed to the present day deterministic runs.

570 For STRATOS, the focus is on continuing work done in relation to  
571 distribution/production maps (Thørring et al., 2010) and to include <sup>90</sup>Sr into the model. Such  
572 information is highly important in relation to vulnerability/preparedness – and for evaluating  
573 potential economic consequences of a particular fallout.

574 The long-term marine dispersion of historic <sup>99</sup>Tc discharges from Sellafield has been  
575 studied by Simonsen et al (2017), where the Lagrangian dispersion was modeled off-line,  
576 using the ROMS-TRACMASS model system (See Appendix A.1.6). Here, it was shown that  
577 increasing the model resolution improved the agreement with observations. It was also shown  
578 that a tidal forced Lagrangian drift could only be resolved in the simulations with relatively  
579 high resolution. This Lagrangian drift was particularly strong in the Irish Sea, heading  
580 northwards in those waters. The Lagrangian drift in the Irish Sea was found to impact  
581 the estimated activity concentration as far as in the Barents Sea. As element speciation and  
582 transformation processes are essential for marine transport, further work to include this in the  
583 ROMS-TRACMASS model has been achieved (Simonsen et al., 2019).

584 Sensitivity analysis has shown that a series of factors will contribute to the overall  
585 uncertainty in the INCA-RAD output. The analysis has shown that the initial value used for  
586 suspended particulate matters (mg L<sup>-1</sup>) has probably been too high overestimating the  
587 sediment concentration of <sup>137</sup>Cs (Lin et al., 2019). The status of the INCA-RAD model at  
588 NIVA/CERAD is that the whole suite of INCA models will be subject to re-coding. A key  
589 issue is to implement a proper element speciation code including transformation processes  
590 that would affect the river transport and the input to estuarine zones.

591 The results of the implementation of a kinetic model for bioaccumulation processes  
592 into the NRPA box model (Iosjpe et al., 2016) clearly demonstrated that there is a significant  
593 quantitative difference between the kinetic modelling approach and the approach based on the  
594 constant concentration ratios. It is noteworthy that such differences can be observed over



595 relatively long time periods. For example, the maximum differences between the two  
596 approaches can be seen 3, 4 or 5 years after start of the releases depending on scenario. It  
597 clearly shows that kinetic modelling of the bioaccumulation processes can provide a more  
598 correct description of the concentration of radionuclides in biota. Results also demonstrate  
599 that kinetic modelling of bioaccumulation processes leads to a better harmonisation between  
600 the different calculations (for example, between doses to the critical group and concentrations  
601 in marine organisms for short-life radionuclides) and to better logical explanations of the  
602 results.

603         The ERICA Tool is under a continued state of development, the latest publication  
604 describing improvements have been given in Brown et al. (2016b). A conspicuous limitation  
605 of the model is linked to the assumption of steady state distribution coefficients and constant  
606 transfer factors (concentration ratios) under conditions when ambient radionuclide activity  
607 concentrations are known to be changing rapidly with time. Recent work has involved the  
608 development of biokinetic models to more realistically account for the dynamics of food-  
609 chain transfer and as exemplified for particular cases involving instantaneous releases from  
610 dumped nuclear objects in the Arctic (Brown et al., 2016a); (Hosseini et al., 2017). Such  
611 models can be simply linked to components of the ERICA Tool to provide estimates of the  
612 environmental exposures and associated dynamics as demonstrated in the aforementioned  
613 publications.

614

## 615 4 Conclusions and further work

616         Predicted impacts from hypothetical, yet realistic, scenarios are important in  
617 emergency preparedness work to scale the necessary emergency plans, response strategies  
618 and measurement capacities. Our study has shown that using specialized and generic models  
619 together with DSS in a chain is useful to predict possible impacts from a large fallout of <sup>137</sup>Cs

620 over Norwegian territories. We used a combination of the ARGOS DSS and its modules  
621 (FDMT) and other modelling codes developed for Norwegian conditions (SNAP, NRPA box  
622 model, INCA-RAD, STRATOS) or of a generic character (ROMS, ERICA Tool) to predict  
623 activity concentrations and doses / dose rates to both humans and the environment via various  
624 exposure routes.

625         In the pre- or early accident phases, rapid assessment of possible impacts are  
626 necessary to take the right decisions to protect life, health and societal interests. DSS like  
627 ARGOS and RODOS, coupled with national meteorological atmospheric dispersion models,  
628 are very valuable for rapid support to decision makers for protecting people and the  
629 production of food, feed and goods. In these phases, decisions need to be taken within hours  
630 or 1-2 days. For other impacts, such as contamination of aquatic areas, forests and  
631 recreational areas, and likewise long-term consequences for food production systems, the  
632 decision makers have more time to decide. Time would allow the use of various regionally  
633 adapted models in combination with predicted deposition and measurement results before  
634 deciding on the necessary countermeasures. These models could, of course, be modules in a  
635 DSS that have been adapted to a region or country, or they could be national models  
636 developed specifically for an ecosystem and/or a region. Our study has shown that a chain of  
637 different regional/national models works well in combination with ARGOS DSS and could  
638 be used to assess impacts in a variety of ecosystems.

639         The modelled activity concentrations and doses / dose rates can be used further in  
640 optimising countermeasures for various sectors and ecosystems e.g., using the AgriCP  
641 module for agricultural countermeasures, or performing cost-benefit analyses for remediation  
642 actions. Recently, a cost-benefit analysis framework was adapted to radioactively  
643 contaminated sites and tested on a site contaminated by naturally occurring radionuclides in

644 the Euratom TERRITORIES<sup>2</sup> project (Liland et al., 2019). This framework will now be used  
645 for evaluating agricultural countermeasures for this hypothetical Sellafield scenario.

646 The choice between a fully-fledged DSS with specific modules for all ecosystems or a  
647 combination of DSS modules and regional/national models, needs to be taken on a national  
648 level by the relevant experts. The suitability of the former and the resources needed for  
649 regional/national adaptation of parameter values, must be evaluated compared to the latter.  
650 The need for specific regional/national models could be more prominent for some countries,  
651 for instance marine models in Norway where fisheries and aquaculture are important for diet,  
652 employment and export. In any case, the modelling tools need to be set up and tested before  
653 an accident happens, if they are to have any value in a crisis management situation.

654 Last, but not least, CERAD will continue the effort of reducing model uncertainties to  
655 improve our health and environmental impact assessment tools for future nuclear accidents.

656

657 **Funding:** This work was partly funded by the Research Council of Norway (RCN) through  
658 its Centres of Excellence funding scheme, project number 223268/F50. Additional funding  
659 was provided through the Euratom COMET project, EC contract number 604974 and RCN  
660 project number 230295.

661

---

<sup>2</sup> To Enhance uncertainties Reduction and stakeholders Involvement Towards integrated and graded Risk management of humans and wildlife In long-lasting radiological Exposure Situations (<https://territories.eu/>)

662 **Appendix 1 – Description of DSS and models used to assess the impacts in**  
663 **Norway from a hypothetical accident scenario at the Sellafield site.**

664 **A.1.1 SNAP atmospheric dispersion and deposition**

665 SNAP is a Lagrangian particle model developed at MET Norway (Saltbones et al.,  
666 1996). It simulates transport and deposition of radioactivity from an atmospheric plume of  
667 radioactive contaminants. The input data are the source term (activity in Bq, particle size and  
668 density) for the released radionuclides, the accident site coordinates, the release height and  
669 release time. The emitted mass of radioactivity is distributed among a large number of model  
670 particles. After the release, each model particle carries a given amount of the radioactive  
671 substances which can be in the form of a gas, a noble gas, aerosols or particles. Although  
672 aerosols and particles of varying size and density can be included in the model, only aerosols  
673 were assumed in the present work. The HIRLAM<sup>3</sup> and ECMWF<sup>4</sup> models are used as the  
674 meteorological input provider for SNAP.

675 The atmospheric boundary layer can have different depths usually ranging from 300 to  
676 2500 m and the model assumes instantaneous and homogenous mixing of particles within the  
677 layer.

678 The basic outputs from the dispersion modelling are air concentration ( $\text{Bq m}^{-3}$ ), time  
679 integrated air concentration ( $\text{Bq}\cdot\text{h m}^{-3}$ ), and deposition on ground ( $\text{Bq m}^{-2}$ ). This information  
680 is given for each isotope of interest, and over a time period which is covered by the available  
681 meteorological forecast.

---

<sup>3</sup>HIRLAM, the High Resolution Limited Area Model, is a [Numerical Weather Prediction](https://en.wikipedia.org/wiki/HIRLAM) (NWP) forecast system developed by European meteorological institutes (<https://en.wikipedia.org/wiki/HIRLAM>)

<sup>4</sup> ECMWF, European Centre for Medium-Range-Weather Forecasts

682           The model version for the present simulation (Bartnicki et al., 2011) used  
683 meteorological data from the HIRLAM model with a spatial resolution of approximately 10  
684 km x 10 km.

685

### 686 **A.1.2 ARGOS decision support system**

687           ARGOS is a decision support system designed for response to nuclear and  
688 radiological accidents (Hoe et al., 2009). Its main purpose is to provide a set of tools which  
689 can help in assessing the consequences of an accident both prior to a release (predictive) and  
690 after. The main tools in ARGOS are dispersion modelling, management of measurement data  
691 and impact assessments in agricultural and urban areas. Furthermore, ARGOS contains a  
692 database of nuclear reactors including reactor inventory, source terms, radionuclides, dose  
693 conversion factors, population data etc. ARGOS supports different atmospheric dispersion  
694 models. Such models require access to large Numerical Weather Predictions (NWP) data and,  
695 in some cases, super computers to do the modelling. Thus, long range runs are done on  
696 remote servers often hosted by meteorological institutes. MET Norway provides this service  
697 through the long range model SNAP which is integrated with ARGOS. The ARGOS operator  
698 defines the position and amount of radioactive material released into the air over time (source  
699 term) and sends a request through ARGOS to MET Norway to perform dispersion  
700 calculations with SNAP. The results are received in ARGOS within 15 minutes.

701           The outputs are raster files with resolution in this work of 10x10 km on total deposition  
702 and concentrations in air ( $\text{Bq m}^{-3}$ ,  $\text{Bq}\cdot\text{h m}^{-3}$ ) which ARGOS uses to calculate other  
703 aggregated outputs like dose to thyroid (if iodine is present), total effective dose, dose rate  
704 etc. With a good numerical estimate of the source term, the output from dispersion models  
705 can give an early assessment of potential consequences for humans following a nuclear  
706 accident.

707 It should be noted that the direct combination of SNAP through ARGOS DSS only  
708 works for recent and forecasted weather situations. For historic weather situations as used for  
709 this work, SNAP had to be started offline from the ARGOS DSS.

710

### 711 ***A.1.3 FDMT food chain modelling***

712 FDMT is used in the Decision Support Systems ARGOS and RODOS to simulate  
713 transfer of radioactive substances in food chains following radioactive fallout. The user can  
714 select radioactive isotopes from 26 elements.

715 FDMT is based on the ECOSYS dynamic model developed in the early 1990's (Müller  
716 and Pröhl, 1993). Based on input data on deposition to soils and vegetated soils ( $\text{Bq m}^{-2}$ ) and  
717 air concentrations ( $\text{Bq m}^{-3}$ ), radionuclide concentrations in food and feedstuffs ( $\text{Bq kg}^{-1}$ ) can  
718 be calculated for a chosen time period, from days to years. It includes a number of processes  
719 such as interception, translocation, weathering, root uptake, growth dilution, processing of  
720 feedstuffs, transfer to animal products, and processing of foodstuffs.

721 A large number of adjustable parameters are included in the module where some are  
722 dependent on site and situation, whereas others have a more general validity. A regional  
723 adaptation of these parameters is recommended as many of the default values are  
724 representative for Southern Germany. For a detailed description of FDMT parameters  
725 including default values reference is given to e.g., Müller et al. (2004).

726 A range of products are included in the model: feed stuffs such as grass, hay and maize;  
727 edible plants such as varieties of leafy vegetables, root vegetables and cereals; animal  
728 products (milk, meat, eggs); and processed food such as cheese, butter and beer. By also  
729 including a defined human diet, FDMT can calculate ingestion doses to humans (mSv) for  
730 various age groups, from infants to adults, over a chosen time period.

731

732 ***A.1.4 STRATOS pasture and wild foodstuffs modelling***

733 STRATOS (Thørring et al., 2010) is a terrestrial model developed by the Norwegian  
 734 Radiation and Nuclear Safety Authority to predict long term impacts on wild foodstuffs and  
 735 rough grazing animals in Norway, i.e., wild berries, mushrooms, game, reindeer, lamb, and  
 736 goat milk – foodstuffs not presently covered by FDMT in a satisfactory way. It is a screening  
 737 model with the purpose of distinguishing between areas where food intervention levels might  
 738 be exceeded and areas where they are not. The model incorporates information on (a)  
 739 deposition of <sup>137</sup>Cs and <sup>134</sup>Cs, (b) aggregated transfer factors (T<sub>ag</sub>) for Cs to vegetation or  
 740 animals, (c) Norwegian food intervention levels, and (d) geographical information on  
 741 distribution of grazing animals / hunting statistics.

742 The aggregated transfer factor is defined as the ratio between the activity concentration  
 743 in a given animal or plant (Bq kg<sup>-1</sup> fresh weight) and the total deposition density in the  
 744 grazing area (Bq m<sup>-2</sup>). Uncertainty/variability regarding transfer is reflected in the model by  
 745 using three different T<sub>ag</sub>: minimum, expected and maximum. The values used are based on  
 746 Norwegian post-Chernobyl research, see Table A.1, and are generic for the whole of Norway  
 747 without regional specific values.

748

749 *Table A.1: Aggregated transfer factors used in the STRATOS model (Thørring et al., 2010).*

Product	Harvest period	Transfer factor		
		Expected	min	max
Wild berries	Jul-Sep	0.007	0.0003	0.04
Mushrooms	Jul-Oct	0.02	0.0005	0.2
Moose	Sep-Nov	0.02	0.005	0.2
Red deer	Sep-Nov	0.02	0.005	0.2
Roe deer	Oct-Des	0.05	0.005	0.2
Reindeer	Late Oct-Mar	0.25	0.05	1.5
Reindeer	Sep-early Oct	0.15	0.05	0.5
Lamb	Oct-Des	0.04	0.01	0.2
Goat milk	Jun-Sep	0.007	0.001	0.02

750 The maximum  $T_{ag}$  can typically be representative of the first period after an accident or  
751 for particularly vulnerable areas. The expected transfer factor is the most likely transfer based  
752 on the existing amount of data. If the food activity concentration exceeds the food  
753 intervention level using this  $T_{ag}$ , it means that countermeasures will probably be necessary for  
754 many years. The minimum  $T_{ag}$  may be interpreted as being representative of areas of very  
755 low sensitivity to radioactive caesium and/or for the situation decades after an accident. If the  
756 results from a model run shows that the food intervention level is exceeded in a given area  
757 using the minimum  $T_{ag}$ , the foodstuff will probably exceed the intervention level for many  
758 years, even decades.

759 The model does not include an explicit time function. The estimations of how long the  
760 contamination of a given foodstuff will be above the food intervention level is based on the  
761 range of  $T_{ag}$ 's from min to max.

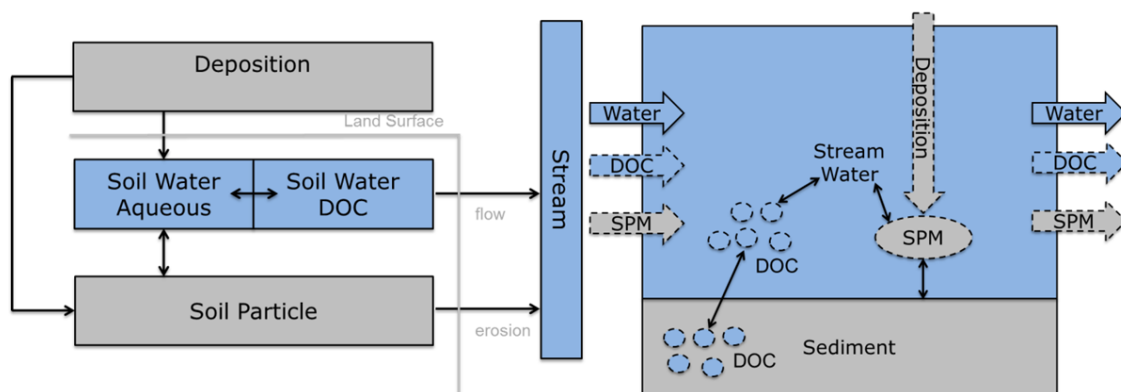
762 Activity concentrations can be coupled with geographical information on the number of  
763 grazing or hunted animals to estimate the proportion of the annual production that is  
764 exceeding intervention levels for a given area.

### 765 ***A.1.5 INCA-RAD freshwater modelling***

766 The INCA (INtegrated CAtchment model) family of codes include a set of tools aimed at  
767 predicting hydrological and biogeochemical processes controlling lateral transfer of nutrients  
768 such as sodium, phosphorus and carbon (Futter et al., 2007); (Wade et al., 2004); (Whitehead  
769 et al., 2011), and environmental contaminants such as mercury (Futter et al., 2012) from soils  
770 to rivers, as well as riverine transport and sediment dynamics as a function of climate,  
771 hydrology and land use. A new synthesis model - INtegrated CAtchment model for  
772 RADionuclides (INCA-RAD) was developed to integrate several features of previous INCA  
773 models and adding the capability of simulating and predicting the transport and retention of  
774 radionuclides in river basins at catchment-scale and in daily time steps. INCA-RAD contains



775 a rainfall-runoff hydrological module, a sediment transport and particle erosion module, a  
 776 biogeochemical cycling module, and a radionuclides geochemistry module. Based on user-  
 777 defined land-use type and river stretches geometry, and using time series of radionuclides  
 778 deposition ( $\text{Bq m}^{-2}$ ) as inputs, INCA-RAD simulates the temporal variation in radionuclides  
 779 export from different land-use types within a river system, as controlled by reactive transport  
 780 and by radioactive decay. INCA-RAD is able to simulate the transport of radioactive  
 781 elements in several phases, such as dissolved phase, associated with suspended particles and  
 782 bed sediment. A summary of the main mass transfer pathways is presented in Figure A.1.  
 783 Combined with the hydrological simulations, INCA-RAD outputs the radionuclide  
 784 concentrations in the water phase, the particulate phase and the river bed sediment. Aggregate  
 785 values, such as annual flux of radionuclides at a catchment's outlet are also computed and  
 786 utilized as input to marine models.



787  
 788 *Figure A.1: Summary of the main mass transfer pathways in the INCA-RAD model. DOC = Dissolved Organic Carbon, SPM*  
 789 *= Soil Particulate Matter.*

### 790 **A.1.6 ROMS marine dynamic modelling**

791 The Regional Ocean Model System (ROMS, <http://myroms.org>) is a three-dimensional,  
 792 free-surface, Boussinesq, hydrostatic ocean circulation model (Haidvogel et al., 2008). The  
 793 model is an open-source software, with numerous users and application areas. At MET  
 794 Norway, the model is used in the operational ocean forecasting system, as well as for

795 research purposes within ocean modelling. In the operational MET Norway system, this  
796 model system is set up in a production line with different configurations: from a regional  
797 model with 4 km x 4 km resolution covering the Nordic Seas to an 800 m x 800 m model  
798 covering the Norwegian coastal waters.

799 In the dispersion simulations for radioactive discharges in ROMS used in this study, the  
800 radionuclides are assumed to be non-reactive, conservative and totally dissolved.  
801 Consequently,  $^{137}\text{Cs}$  was computed as a tracer that follows the three-dimensional ocean  
802 currents passively. Interaction with sediments and suspended particles was not considered in  
803 this experiment, even if we know that this is an over-simplification that causes relatively  
804 large uncertainties (Simonsen et al., 2019). Computation of the tracer dispersion is performed  
805 on-line simultaneously with the ocean model.

806 In addition to the on-line simulations with ROMS, an off-line dispersion model,  
807 TRACMASS ([www.tracmass.org](http://www.tracmass.org)) is used for simulations of particle transport paths. A finite  
808 number of numerical particles are released in the model, according to a given discharge  
809 scenario. The release can be a spatial distribution, and/or a time-dependent function.  
810 Transport of the particles is computed from the previously simulated ocean model velocity  
811 fields from the hydrodynamic ocean model (ROMS). The spatial resolution will depend on  
812 the output from the ocean circulation model. Each numerical particle will represent a given  
813 activity. The concentration of radioactivity in sea water can be computed from the density of  
814 particles in a certain water volume.

815 We considered two sources for  $^{137}\text{Cs}$  in this marine model: atmospheric fallout and  
816 riverine input. The atmospheric fallout was modelled as an instantaneous deposition on 22  
817 October 2008, which corresponds to the accumulated wet and dry deposition the three first  
818 days after the hypothetical accident. The surface deposition is distributed vertically into the  
819 water column by:

820

$$C(z) = C_0 e^{\frac{z}{\lambda}}$$

821

Equation A.1

822

823 where  $C_0$  is surface concentration,  $z$  is water depth (a negative number) and  $\lambda$  is an e-folding  
824 depth, here chosen to be 4 m. In addition to marine surface deposition, riverine input of  $^{137}\text{Cs}$   
825 can be included as point sources with a time-dependent flux of  $^{137}\text{Cs}$  into the marine model.

826 The outputs are dynamic activity concentrations in sea water ( $\text{Bq m}^{-3}$ ) at various  
827 depths for the chosen time period.

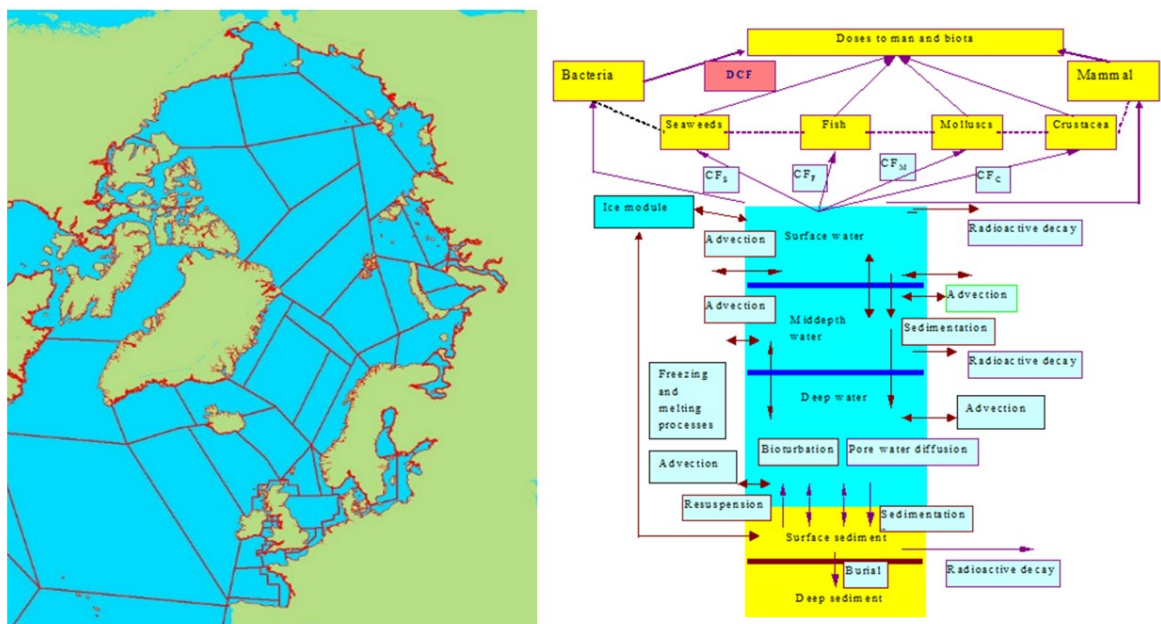
828

### 829 **A.1.7 NRPA marine box model**

830 The marine box model developed at NRPA uses a modified approach for compartmental  
831 modelling which allows for dispersion of radionuclides over time based on either point source  
832 discharges or deposited radionuclides on the surface as input data. It assumes instantaneous  
833 and uniform mixing of radionuclides within the total box volume. The box structures (Figure  
834 A.2, left) for surface, mid-depth and deep water layers have been developed based on  
835 description of polar, Atlantic and deep waters in the Arctic Ocean and the Northern Seas and  
836 site-specific information for the boxes generated from the 3D hydrodynamic model NAOSIM  
837 (Karcher and Harms, 2000).

838 The volume of the three water layers in each box has been calculated using detailed  
839 bathymetry together with GIS. The box model includes the processes of advection of  
840 radioactivity between compartments, sedimentation, diffusion of radioactivity through pore  
841 water in sediments, resuspension, mixing due to bioturbation, particle mixing, and a burial  
842 process of radioactivity in deep sediment layers (Figure A.2, right). Radioactive decay is

843 calculated for all compartments. The output is radionuclide seawater and pore water  
 844 concentrations ( $\text{Bq m}^{-3}$ ) and sediment concentrations ( $\text{Bq kg}^{-1}$ ). In addition, the model  
 845 calculates contamination of marine organisms ( $\text{Bq kg}^{-1}$ ) based on concentrations ratios (CR)  
 846 which is the ratio of concentration in the organism tissue (fresh weight) to that in water (IAEA,  
 847 2004). Dose rates to biota ( $\mu\text{Gy h}^{-1}$ ) are then calculated using dose conversion factors. Doses  
 848 to man can be calculated from the concentration in biota and data for human consumption in  
 849 the respective areas. More detailed descriptions are given in Iosjpe et al. (2002), Iosjpe (2006)  
 850 and Iosjpe et al. (2009).



851  
 852 *Figure A.2: The division of ocean areas in compartments (left) and processes included (right) in the NRPA marine box model*

853 ***A.1.8 The ERICA Tool environmental risk assessment***

854 The ERICA Tool (Brown et al., 2008) provides a means for calculating radiological  
 855 environmental risk based on input data either in the form of discharges to the environment or  
 856 from radionuclide activity concentrations measured in biota and environmental media (e.g.,  
 857 water, sediment). It includes default values for a suite of radioisotopes from 31 elements

858 selected to cover a wide variety of conceivable exposure situations, including accidental  
859 releases.

860 The models used to quantify transfer from water to plants and animals are simple in  
861 nature having been based upon concentration ratios (CR) with an implicit assumption of  
862 equilibrium (steady state conditions for radionuclides between abiotic and biotic  
863 compartments). Similarly, sediment activity concentrations are derived using distribution  
864 coefficients ( $K_d$ 's) derived from various compendia e.g., IAEA (2010). The underlying  
865 transfer databases have been updated to be compatible with comprehensive international  
866 compilations documenting these parameters (Coppelstone et al., 2013). The concentration  
867 values are coupled to occupancy factors and internal and external dose conversion factors to  
868 calculate total dose rates ( $\mu\text{Gy h}^{-1}$ ) to a selection of reference organisms.

869 The Tool uses a default screening dose rate of  $10 \mu\text{Gy h}^{-1}$  applicable to incremental  
870 exposures. The derivation of this value is described in Garnier-Laplace et al. (2008). For dose  
871 rates below  $10 \mu\text{Gy h}^{-1}$  the environmental risk is arguably negligible (Brown et al., 2008),  
872 while dose rates above this screening value indicates that a more detailed assessment with  
873 site-specific data should be performed to determine the potential environmental risk.

874

875 **Appendix 2 – Estimation of the inventory in the HASTs and the source**  
876 **term**

877 The vitrified waste comes in canisters that equates to 10 TeU (‘Tonnes equivalent  
878 Uranium’) of spent fuel (Nuclear Decommissioning Authority, 2010). The activity of  
879 different nuclides in such a canister is given by e.g., Chubu Electric Power (2014), a  
880 company who receives vitrified waste from Sellafield Ltd after reprocessing of spent  
881 Japanese nuclear fuel. In their press release, we find that for  $^{137}\text{Cs}$  we have  $3.0 - 4.7 \cdot 10^{15}$  Bq  
882 per canister. Prognoses from a meeting between the Norwegian Radiation Protection  
883 Authority and the Nuclear Decommissioning Authority (NDA) in June 2013 show an  
884 expected stock of about 6300 TeU of HAL for April 2014. With 10 TeU/canister, this  
885 amounts to 630 canisters. The total amount of  $^{137}\text{Cs}$  is therefore approximately  $1.9 - 3.0 \cdot 10^{18}$   
886 Bq. This agrees well with the plans and signals given by the NDA.

887 We have not done any probability calculations for a possible accident scenario, be it  
888 the loss of cooling, a natural disaster or a malevolent act. We just assume that there will be  
889 loss of the HAL tanks’ integrity and that 1% of all the estimated  $^{137}\text{Cs}$  in the tanks is released  
890 to the air ( $3.0 \cdot 10^{16}$  Bq) as an aerosol at a height where it can be mixed with the atmosphere  
891 and then transported to Norway by atmospheric dispersion.

892 Only  $^{137}\text{Cs}$  was included in the pilot study described. It should be noted that the HAL  
893 contains other long-lived radionuclides besides  $^{137}\text{Cs}$  that would add to the problem.  $^{90}\text{Sr}$  and  
894  $^{90}\text{Y}$  are present in the liquid waste at the same order of magnitude as  $^{137}\text{Cs}$ .  $^{241}\text{Am}$  is present  
895 in quantities between 1 and 10 %,  $^{244}\text{Cm}$  and  $^{154/155}\text{Eu}$  around 1% while other radionuclides  
896 are all in the range 0.001-0.1 % of the  $^{137}\text{Cs}$  content (Chubu Electric Power, 2014).  
897 Americium and curium are transuranium elements that exhibit low transfer in the terrestrial  
898 foodwebs. For instance, in IAEA TRS472 (IAEA, 2010) the recommended gastrointestinal  
899 fractional absorption values for ruminants are 1 for Cs, 0.3 for Sr and 0.0005 for Am and Cm.

900 Similar differences are apparent for transfer factors from soil to plant and transfer coefficients  
901 to milk and meat. Data are scarce for yttrium (Y) and europium (Eu), but the latter is one of  
902 the lanthanides known to exhibit low transfer in terrestrial ecosystems, and Y is a transition  
903 metal with similar chemical properties as the lanthanides.  $^{241}\text{Am}$ ,  $^{244}\text{Cm}$ ,  $^{154/155}\text{Eu}$  and  $^{90}\text{Y}$   
904 would thus be of minor importance compared to  $^{137}\text{Cs}$  and  $^{90}\text{Sr}$  when it comes to terrestrial  
905 food chain transfer. The two latter are elements that resembles the essential elements  
906 potassium (K) and calcium (Ca) that are important nutrients in all living matter, contributing  
907 to a significantly higher transfer of these elements in terrestrial foodwebs.

908

## 909 **References**

- 910 Avila R, Beresford N, Agüero A, Broed R, Brown J, Iospje M, et al. Study of the uncertainty  
911 in estimation of the exposure of non-human biota to ionising radiation. *Journal of*  
912 *Radiological Protection* 2004; 24: A105.
- 913 Backe S, Bjerke H, Rudjord AL, Ugletveit F. Cesium fallout in Norway after the Chernobyl  
914 accident. Statens Inst. for Straalehygiene, 1986.
- 915 Bartnicki J, Haakenstad H, Hov Ø. Operational SNAP model for remote applications from  
916 NRPA. Norwegian Meteorological Institute. Report 2011: 12-2011.
- 917 Brittain JE, Gjerset JE. Long-term trends and variation in  $^{137}\text{Cs}$  activity concentrations in  
918 brown trout (*Salmo trutta*) from Øvre Heimdalsvatn, a Norwegian subalpine lake. The  
919 subalpine lake ecosystem, Øvre Heimdalsvatn, and its catchment: local and global  
920 changes over the last 50 years. Springer, 2010, pp. 107-113.
- 921 Brown J, Amundsen I, Bartnicki J, Dowdall M, Dyve J, Hosseini A, et al. Impacts on the  
922 terrestrial environment in case of a hypothetical accident involving the recovery of the  
923 dumped Russian submarine K-27. *Journal of environmental radioactivity* 2016a; 165:  
924 1-12.
- 925 Brown JE, Alfonso B, Avila R, Beresford NA, Copplestone D, Hosseini A. A new version of  
926 the ERICA tool to facilitate impact assessments of radioactivity on wild plants and  
927 animals. *Journal of Environmental Radioactivity* 2016b; 153: 141-148.
- 928 Brown JE, Alfonso B, Avila R, Beresford NA, Copplestone D, Pröhl G, et al. The ERICA  
929 Tool. *Journal of Environmental Radioactivity* 2008; 99: 1371-1383.
- 930 Chubu Electric Power. Regarding the Application for Confirmation of External Disposal of  
931 Returned Vitrified Waste. Chubu Electric Power, Japan, 2014.
- 932 Copplestone D, Beresford NA, Brown J, Yankovich T. An international database of  
933 radionuclide concentration ratios for wildlife: development and uses. *Journal of*  
934 *environmental radioactivity* 2013; 126: 288-298.
- 935 Futter M, Butterfield D, Cosby B, Dillon P, Wade A, Whitehead P. Modeling the  
936 mechanisms that control in-stream dissolved organic carbon dynamics in upland and  
937 forested catchments. *Water Resources Research* 2007; 43.

938 Futter M, Poste A, Butterfield D, Dillon P, Whitehead P, Dastoor A, et al. Using the INCA-  
939 Hg model of mercury cycling to simulate total and methyl mercury concentrations in  
940 forest streams and catchments. *Science of the total environment* 2012; 424: 219-231.

941 Garnier-Laplace J, Copplestone D, Gilbin R, Alonzo F, Ciffroy P, Gilek M, et al. Issues and  
942 practices in the use of effects data from FREDERICA in the ERICA Integrated  
943 Approach. *Journal of Environmental Radioactivity* 2008; 99: 1474-1483.

944 Haidvogel DB, Arango H, Budgell WP, Cornuelle BD, Curchitser E, Di Lorenzo E, et al.  
945 Ocean forecasting in terrain-following coordinates: Formulation and skill assessment  
946 of the Regional Ocean Modeling System. *Journal of Computational Physics* 2008;  
947 227: 3595-3624.

948 Hansen HS, Nielsen SP, Andersson KG, Thørring H, Joensen HP, Isaksson M, et al. Effect of  
949 Nordic diets on ECOSYS model predictions of ingestion doses. *Radiation protection*  
950 *dosimetry* 2010; 140: 182-190.

951 Hoe S, McGinnity P, Charnock T, Gering F, Jacobsen LHS, Sørensen JH, et al. ARGOS  
952 decision support system for emergency management. *Proceedings of the 12th*  
953 *International Congress of the International Radiation Protection Association. Buenos*  
954 *Aires, Argentina: IRPA, 2009.*

955 Hosseini A, Amundsen I, Brown J, Dowdall M, Karcher M, Kauker F, et al. Impacts on the  
956 marine environment in the case of a hypothetical accident involving the recovery of  
957 the dumped Russian submarine K-27, based on dispersion of <sup>137</sup>Cs. *Journal of*  
958 *environmental radioactivity* 2017; 167: 170-179.

959 IAEA. Technical reports series no. 422, Sediment Distribution Coefficients and  
960 Concentration Factors for Biota in the Marine Environment. In: Agency IAE, editor.  
961 Technical reports series, Vienna, 2004.

962 IAEA. Handbook of Parameter Values for the Prediction of Radionuclide Transfer in  
963 Terrestrial and Freshwater Environments. Technical Report Series no. 472.  
964 International Atomic Energy Agency, Vienna, 2010.

965 IFE. Målinger av matvarer utført ved IFE Kjeller etter Tsjernobyl-ulykken. Norsk  
966 oppdrettslaks, andre marine produkter. Institute for energy technology, IFE, 1986.

967 Iosjpe M. Environmental modeling: Modified approach for compartmental models. In: Povinec  
968 PP, Sanchez-Cabeza JA, editors. *Radionuclides in the Environment: International*  
969 *Conference on Isotopes in Environmental Studies: Aquatic Forum 2004, 25-29*  
970 *October, Monaco. 8. Elsevier Science Limited, 2006, pp. 463-476.*

971 Iosjpe M. A sensitivity analysis of the parameters controlling water-sediment interactions in  
972 the coastal zone: Consequences to man and environment. *Journal of Marine Systems*  
973 2011; 88: 82-89.

974 Iosjpe M, Brown J, Strand P. Modified approach to modelling radiological consequences  
975 from releases into the marine environment. *Journal of Environmental Radioactivity*  
976 2002; 60: 91-103.

977 Iosjpe M, Isaksson M, Joensen H, Jonsson G, Logemann K, Roos P. Effects of dynamic  
978 behaviour of Nordic marine environment to radioecological assessments, 2016, ISBN:  
979 ISBN 978-87-7893-442-0. NKS-B reports. Nordic Nuclear Safety Research,  
980 Copenhagen, 2016.

981 Iosjpe M, Liland A. Evaluation of environmental sensitivity of the marine regions. *Journal of*  
982 *Environmental Radioactivity* 2012; 108: 2-8.

983 Iosjpe M, Logemann K. Radioecological Assessment after Potential Accident with the  
984 Modern Operative Nuclear Submarine in the Nordic Marine Environment. ,  
985 Goldschmidt conference, 8-13 June, 2014, Sacramento, USA, 2014, pp. 1092.



986 Iosjpe M, Reistad O, Amundsen I. Radioecological consequences of a potential accident  
 987 during transport of spent nuclear fuel along an Arctic coastline. *Journal of*  
 988 *environmental radioactivity* 2009; 100: 184-191.  
 989 Karcher M, Harms I. Estimation of water and ice fluxes in the Arctic for an improved box  
 990 structure of the NRPA box model (Transport Programme). Report to the Norwegian  
 991 Radiation Protection Authority (NRPA), 2000.  
 992 Klein H, Bartnicki J, Dyve J. Improved source term description in Eulerian models in  
 993 ARGOS. *RADIOPROTECTION* 2016; 51: S125-S127.  
 994 Komperød M, Friberg E, Rudjord A. Radiation Doses to the Norwegian Population.  
 995 Summary of radiation doses from planned exposure and the environment.  
 996 StrålevernRapport. StrålevernRapport 2015:13. Norwegian Radiation Protection  
 997 Authority, Østerås, 2015.  
 998 Komperød M, Østmo T, Skuterud L. Radioactivity in Norwegian Food - Results of the  
 999 monitoring of animals and food 2016. In: Authority NRP, editor. StrålevernRapport.  
 1000 2017:10. Norwegian Radiation Protection Authority, Østerås, Norway, 2017.  
 1001 Landman C, Päsler-Sauer J, Raskob W. The decision support system RODOS. *The Risks of*  
 1002 *Nuclear Energy Technology*. Springer, 2014, pp. 337-348.  
 1003 Liland A, Goronovski A, Navrud S, Tkaczyk A, Perez-Sanchez D, Prats SG, et al.  
 1004 Framework for socio-economic analysis. EJP-CONCERT deliverables.  
 1005 TERRITORIES project, 2019, pp. 92.  
 1006 Liland A, Skuterud L. Lessons learned from the Chernobyl accident in Norway. In: Oughton  
 1007 D, Hansson SO, editors. *Social and ethical aspects of radiation risk management*. 19.  
 1008 Elsevier, Oxford, 2013, pp. 159-176.  
 1009 Liland A, Tomkiv Y, Oughton D, Navrud S, Romstad E, Skuterud L. The power of  
 1010 collaborative deliberation in stakeholder dialogue seminars. *Journal of Risk Research*  
 1011 2017: 1-25.  
 1012 Lin Y, Couture R-M, Klein H, Ytre-Eide MA, Dyve JE, Lind OC, et al. Modelling  
 1013 Environmental Impacts of Cesium-137 Under a Hypothetical Release of Radioactive  
 1014 Waste. *Bulletin of environmental contamination and toxicology* 2019: 1-6.  
 1015 Müller H, Gering F, Pröhl G. Model Description of the Terrestrial Food Chain and Dose  
 1016 Module FDMT in RODOS PV6. 0. RODOS (RA3)-TN (03) 06 (2006). Karlsruhe  
 1017 Institute of Technology, Karlsruhe, 2004.  
 1018 Müller H, Pröhl G. ECOSYS-87: A dynamic model for assessing radiological consequences  
 1019 of nuclear accidents. *Health physics* 1993; 64: 232-252.  
 1020 Nordic guidelines and recommendations. Nordic guidelines and recommendations, Protective  
 1021 measures in early and intermediate phases of a nuclear or radiological emergency.  
 1022 The Nordic radiation protection and nuclear safety authorities, 2014, pp. 63.  
 1023 Norwegian Radiation Protection Authority. The Kyshtym accident, 29th September 1957. In:  
 1024 Authority NRP, editor. Norwegian Radiation Protection Authority, 2007.  
 1025 Nuclear Decommissioning Authority. NDA Business Plan 2010–2013. Nuclear  
 1026 Decommissioning Authority, 2010.  
 1027 Pröhl G, Müller H. Data requirements for the adaptation of the ARGOS food chain module  
 1028 for the application at specific sites. . Draft report ConRad – Consulting in  
 1029 Radioecology (version 12.05.2005). , 2005.  
 1030 Raskob W, Hugon M, Jacobsen L, Andersson K, Charnock T, Kaiser J, et al. Implementation  
 1031 in ARGOS of ERMIN and AGRICP. *Radioprotection* 2010; 45: S191-S198.  
 1032 Raskob W, Kerekes A, Dvorzak A, Slavik O, Pecha P. Documentation on the Two INCO  
 1033 Working Programs: Review of the Adequacy of the Present Foodchain and Dose  
 1034 Calculations and Collection of the Data Required for Each Radioecological Region  
 1035 and their Integration into RODOS. RODOS (WG3)–TN (99)–40 2000.

1036 Salbu B. Environmental impact and risk assessments and key factors contributing to the  
1037 overall uncertainties. *Journal of environmental radioactivity* 2016; 151: 352-360.

1038 Saltbones J, Foss A, Bartnicki J. Severe Nuclear Accident Program (SNAP) a Real Time  
1039 Dispersion Model. *Air Pollution Modeling and Its Application XI*. Springer, 1996, pp.  
1040 471-479.

1041 Sandlund OT, Bongard T, Brettum P, Finstad AG, Fjellheim A, Halvorsen GA, et al.  
1042 Nettverk for biologisk mangfold i ferskvann–samlerapport 2010. Atna-og  
1043 Vikedalsvassdragene. NINA rapport, 2010.

1044 Simonsen M, Lind OC, Saetra O, Isachsen PE, Teien HC, Albretsen J, et al. Coastal transport  
1045 of river-discharged radionuclides: Impact of speciation and transformation processes  
1046 in numerical model simulations. *Sci Total Environ* 2019; 669: 856-871.

1047 Strand P, Selnaes T, Bøe E, Harbitz O, Andersson-Sørliie A. Chernobyl fallout: internal doses  
1048 to the Norwegian population and the effect of dietary advice. *Health physics* 1992; 63:  
1049 385-392.

1050 Sørensen JH, Amstrup B, Feddersen H, Korsholm US, Bartnicki J, Klein H, et al.  
1051 Meteorological Uncertainty of atmospheric Dispersion model results (MUD): Final  
1052 Report of the NKS-B MUD activity. NKS-B reports. Nordic nuclear safety reseach,  
1053 Copenhagen, 2014.

1054 Thørring H, Dyve J, Hevrøy T, Lahtinen J, Liland A, Montero M, et al. COMET project  
1055 deliverable COMET IRA-Human-D3: Set of improved parameter values for Nordic  
1056 and Mediterranean ecosystems for Cs-134/137Sr-90, I-131 with justification text.  
1057 European Commission Luxemburg, 2016.

1058 Thørring H, Ytre-Eide M, Liland A. Consequences in Norway after a hypothetical accident at  
1059 Sellafield - predicted impacts on the environment. *StrålevernRapport*.  
1060 *StrålevernRapport 2010:13*. Norwegian Radiation Protection Authority, Østerås,  
1061 2010.

1062 Vives i Batlle J, Wilson R, Watts S, Jones S, McDonald P, Vives-Lynch S. Dynamic model  
1063 for the assessment of radiological exposure to marine biota. *Journal of environmental*  
1064 *radioactivity* 2008; 99: 1711-1730.

1065 Wade A, Neal C, Butterfield D, Futter M. Assessing nitrogen dynamics in European  
1066 ecosystems, integrating measurement and modelling: conclusions. *Hydrology and*  
1067 *Earth System Sciences Discussions* 2004; 8: 846-857.

1068 Whitehead P, Jin L, Baulch H, Butterfield D, Oni S, Dillon P, et al. Modelling phosphorus  
1069 dynamics in multi-branch river systems: a study of the Black River, Lake Simcoe,  
1070 Ontario, Canada. *Science of the Total environment* 2011; 412: 315-323.

1071 Ytre-Eide MA, Standring WJ, Amundsen I, Sickel M, Liland A, Saltbones J, et al.  
1072 Consequences in Norway of a hypothetical accident at Sellafield: Potential release -  
1073 transport and fallout. *StrålevernRapport*. *StrålevernRapport 2009:7*. Norwegian  
1074 Radiaton Protection Authority, Østerås, 2009.

1075